Hokkaido University

Lab of Robotics and Dynamics

Politecnico di Torino

Department of Mechanical and Aerospace engineering

Vibration Energy Harvesting using Piezoelectric Materials.

Master Thesis of:

Mohammad Hamid Raza

Advisor:

Yukinori kobyashi (Hokkaido University)

Stefano Marchesiello(Politecnico di torino)

October 2019

Contents

Table of Figures

Abstract

The Purpose of this study is to analyze the Piezoelectric energy harvesting technology. The different modeling techniques are studied and compared and after studying the literature review, the optimal shape and material of the cantilever beam and piezoelectric patch is chosen to work on.

The Ansys Workbench with the installed piezo and mems extension is used for finite element analysis of the Trapezoidal Cantilevered beam harvester and a command is written in the workbench to connect with the Mechanical ADPL and reading the data output of displacement and voltage for post processing. The voltage output is studied at different resistance loading conditions and to find the optimal resistance of the harvester. The voltage outputs and instantaneous power at different resistances are compared.

Finally, the experimental methods are studied, and the experiment is set in Robotics and Dynamics Lab in Hokkaido University, but due to shortage of time and due to shortage of some experimental equipment the experiment could not be completed.

1. Introduction

In a few applications there is a developing need to control the gadgets which needn't bother with the association of wires and the burden of batteries. In the previous few years there has been a blast of research in the procedures of harvesting or (Scavenging) from encompassing sources. The market of convenient electronic gadgets too the remote sensor hubs has been expanding also in the most recent decade and the energy required to work them has been diminishing in parallel. Along these lines, reaping some portion of squandered mechanical energy from the ambiance has picked up intrigue. Moreover, such energy supply is free, clean and enduring. In fig 1 an overview of already existing techniques is shown taken from (Calio, 2014).

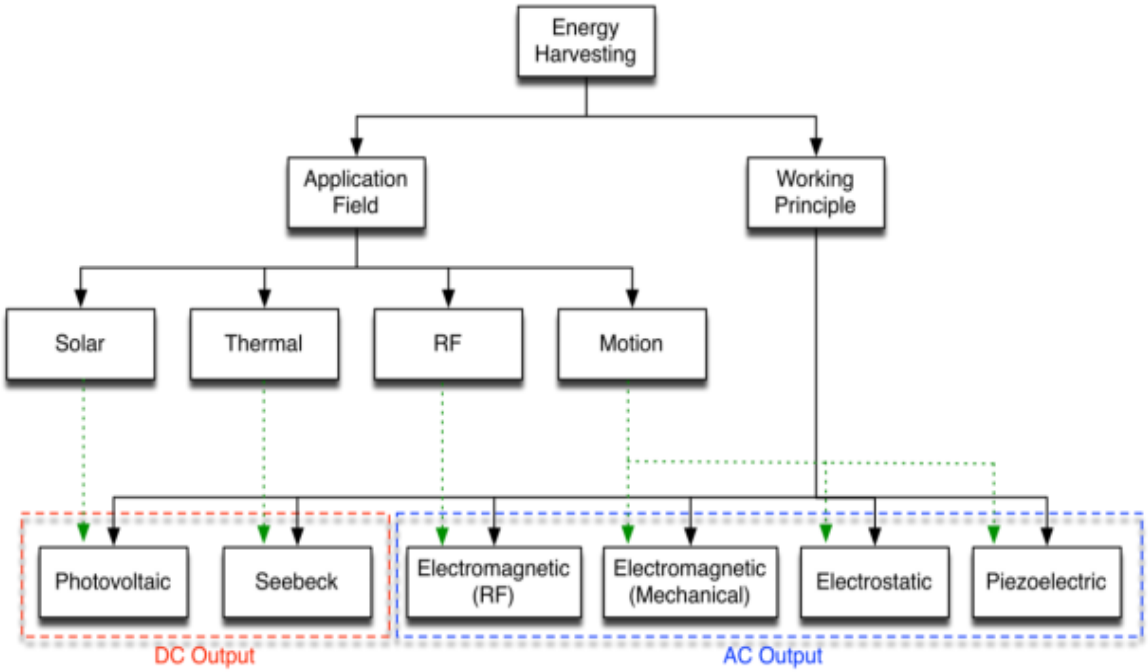

Figure 1. Hierarchy of main energy harvesting technologies

These wireless sensor nodes are capable to operate for a long time and remove the need of batteries if can be powered by any kind of energy harvesting phenomenon. The energy harvesting scheme can be used to convert and store the ambient energy as an electrical energy. There are quite a few sources of wasted energy present in our ambiance. The most common ones used for energy scavenging are Solar, wind, thermal and shallow ground thermal energy etc. In this thesis I will focus on the energy harvesting from wasted vibrations in the atmosphere. The source of wasted vibrations exists all around us in many forms. It can come from the movement of a human body to the vibrations from machinery. The frequency of the vibrations depends on the source, it can range from few Hz in case of Human body motion to few kHz in case of machinery vibrations. There are already quite a few applications of vibration energy harvesters and are growing continuously as the cost keeps getting lower and lower.

Some common applications are the structural monitoring the health of systems with the help of wireless sensor nodes especially the systems which are present in the remote places. To make a good application of these type of systems there should be a continuous source of vibrations, such as in the bridges, airplane wings, trains, railway tracks to monitor the health of a track, helicopters or shafts of the turbomachinery etc. Such systems are always producing vibrations which are wasted, so the idea is to harvest the part of this wasted mechanical energy and convert it into small amount of electrical energy which can be used to power wireless sensor nodes.

2. Literature review

2.1. Wireless Sensor Nodes

As of late, the advancement of distributed wireless sensor systems has been a noteworthy focal point of many research groups. As the systems, which are typically intended to keep running on batteries increment in number and the gadgets decline in size, the substitution of drained batteries isn't reasonable. Techniques for scavenging surrounding power for use by wireless sensor nodes have been investigated to make the wireless nodes and coming about wireless sensor networks inconclusively independent. Such systems could conceivably be utilized for a wide assortment of utilizations. A few possible applications include monitoring temperature, light, and the location of persons in commercial buildings to control the environment in a more energy efficient manner, sensing harmful chemical agents in high traffic areas, monitoring fatigue crack formation on aircraft, monitoring acceleration and pressure in automobile tires, etc. Indeed, many experts foresee that very low power embedded electronic devices will become a ubiquitous part of our environment, performing functions in applications ranging from entertainment to factory automation. Advances in low power DSP's (Digital Signal Processors) and trends in VLSI (Very Large-Scale Integration) system-design have reduced power requirements for the individual nodes. Power consumption of tens to hundreds of µW is predicted and a current milli-scale commercial node has an average power consumption of 6 - 300 µW, depending on the application and/or mode of operation. This lowered power requirement has made self-powered sensor nodes a possibility. To evaluate or develop a power solution for a wireless sensor node, it is imperative to understand the sub-components and power drains of the node. The general architecture and applications of the nodes will be considered first. Next, the power drains of each component will be discussed.

2.2.Architecture and Power drains

To assess the power consumption of nodes, it is important to understand the architecture of wireless sensor nodes. The node can be divided into four subsystems.

- Computing/processing unit (logic)
- Communication unit
- Sensing unit
- Power Supply

The specific application of a wireless sensor node network affects the power consumed by the individual nodes and will influence the power solution(s) chosen for the nodes in the network. For example, high data transfer rates necessitate larger power sources. Each of the node subsystems will be discussed briefly, with the emphasis on power consumption. The Following Figure shows how the simple Energy harvesting scheme works. The ambient energy is converted and stored and is then supplied to Sensor nodes for applications like sensing, actuating or sending wireless signals.

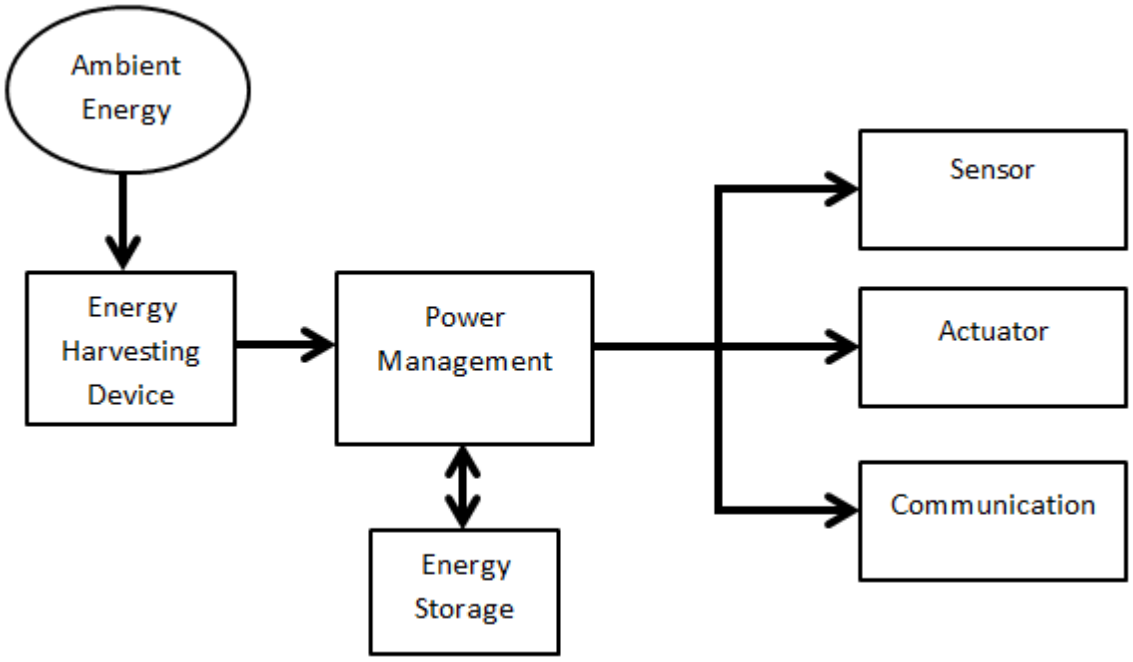

Figure 2 Generic Wireless sensor node architecture

The computing unit includes the memory and a microprocessor or micro-controller (MCU). The power consumption of the MCU changes greatly, depending on the processor used and its operational mode (active, sleep, or idle mode). The processor will in turn depend on the application. For instance, two commonly used processors are the Intel Strongarm and Atmel's

AVR. The Strongarm has an active power consumption of 400 μW, whereas the AVR consumes only 16.5 mW in active mode but has much less processing capability. The consumptions of the Intel processor in its other operational modes are: 50 mW in idle mode and 160 μW in sleep mode. This puts in context power consumptions of 10 - 100 μW that have been predicted.

In the communication unit, Power utilization is be affected by the modulation type, information transmission rate, transmission power, and operational modes. These operational modes incorporate transmit, get, inactive and rest. Exchanging between the modes additionally consumes power as well.

The sensing unit control utilization is hard to survey since there are various sensors accessible and accessible with these hubs. Also, a few nodes incorporate both computerized and analog sources and bolster numerous sensors. Regular power channels incorporate signal inspecting, signal conditioning, and analog to digital transformation (if essential). As indicated by (Raghunathan, Schurgers, Park, & Srivastava, 2002) the power devoured by detached sensors (e.g., accelerometers, thermometers, weight sensors, strain sensors, and so on.) is insignificant when contrasted with different subsystems.

The power source must stimulate the whole sensor hub. To guarantee a steady voltage supply, a DC-DC voltage up-converter might be essential. On account of a battery power source, the voltage diminishes as the rate of the chemical reaction diminishes. For energy scavenging innovations, the source can be discontinuous or at levels beneath the maximum power requirement of the hub. For this situation, a storage device (battery) will be important to fulfil the temporary high-power request and the normal power created ought to be more prominent than the normal power devoured by the node. The power utilised by Rockwell's WINS hubs (most extreme power utilization ~ 1 W, yet normal power expended will be strongly application subordinate) is summarized beneath (Srivastava, 2002):

1. Processor - 30 - 50% of total consumed power.

- Active = 360 mW
- Sleep = 41 mW
- Off = 900 μW

2. Sensor = 23 mW

3. Transceiver = 50 - 70% of total consumed power.

- Transmit vs. processor (active) power = (1 to 2):1 (range dependent)
- Receive vs. processor (active) power = 1:1
- Transmit vs. receive power = 4:3 at maximum range, 1:1 at shorter

range

As the example shows, advances in reduced-power processing and transcribing will drive the realization of effective, self-powered sensor nodes.

2.3.Methods of Powering Wireless sensor networks

There are three possible ways to address the problem of powering the emerging wireless technologies:

- Improve the energy density of storage systems.
- Develop novel methods to distribute power to nodes.
- Develop technologies that enable a node to generate or “scavenge” its own power.

Research to increase the storage density of both rechargeable and primary batteries has been conducted for many years and continues to receive substantial focus. In the following figure the summary of power sources for wireless sensor nodes is shown (Toit, 2005).

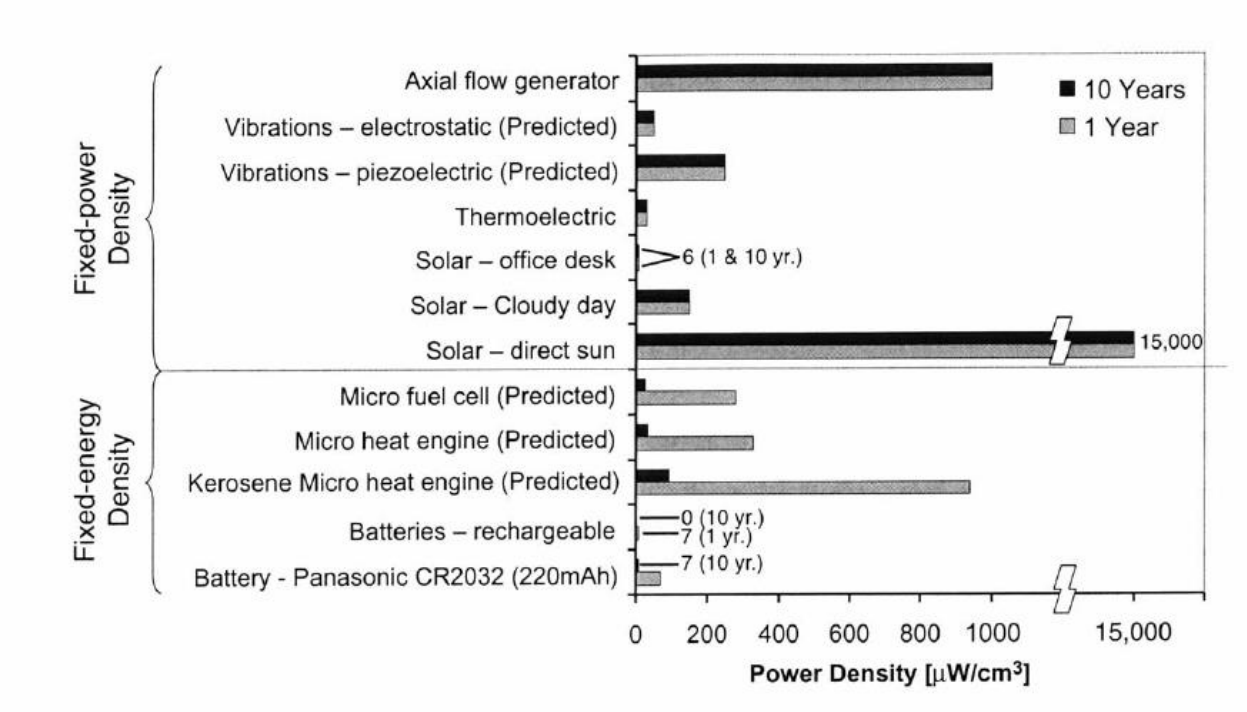

Figure 3 Comparison of power sources for wireless sensor nodes **(Toit, 2005)**

The past few years have additionally observed numerous endeavours to scale down power devices which guarantee a few times the energy density of batteries. At last, more recent research efforts are in progress to create smaller heat engines that guarantee comparative energy densities to fuel cells yet are fit for far higher most extreme power yield. While these innovations guarantee to expand the lifetime of remote sensor hubs, they can't broaden their lifetime uncertainly.

The most widely recognized technique according to (Holger, Willig, & Wolisz, 2004) (other than wires) of distributing power to embedded electronics is utilizing RF (Radio Frequency) radiation.

Numerous passive electronic devices, for example, electronic ID labels are powered by energy rich source a that transmits RF energy to these gadgets, which at that point utilizes that energy to run its hardware. Be that as it may, this technique isn't reasonable when considering dense systems of remote sensor nodes on as a whole space, for example, a room, would should be overwhelmed with RF radiation to supply power to the nodes. The measure of radiation expected to do this would likely exhibit a health danger and today surpasses FCC (Federal Communications Commission) guidelines. For instance, the Location and Monitoring Service (LMS) offered by the FCC works somewhere in the range of 902 and 928 MHz and is utilized as, however not constrained to, a technique to consequently distinguish vehicles (at a toll plaza for example). The amount of power transmitted to a node assuming no interference is given by $\mathbf{P_r = P_0\lambda^2/ (4\pi R^2)}$ where P_0 is the transmitted power, λ is the wavelength of the signal and R is the distance between transmitter and receiver. If a maximum distance of 10 meters and the frequency band of the LMS are assumed, then to power a node consuming 100μW, the power transmitter would need to emit 14 watts of RF radiation. In this band the FCC regulations state that person should not be exposed to more than 0.6 mW/cm^2 (FCC 2002). In the case just described, a person 1 meter away from the power transmitter would be exposed to 0.45 mW/cm^2, which is just under federal regulations. However, this assumes that there are no reflections between the transmitter and receiver. In a realistic situation, the transmitter would need to far more than 14 watts, which would likely put people in the vicinity at risk. The FCC also has regulations determining how much power can be radiated at certain frequencies indoors. For example, the FCC regulation on ceiling mounted transmitters in the 2.4 – 2.4835 GHz band (the unlicensed industrial, scientific, and medical band) is 1 watt (Evans et al 1996), which given the numbers above is far too low to transmit power to sensor nodes throughout a room.

The third strategy is where the Node creates its own power. The thought is that a node would change convert the ambiance energy from the surroundings into power for use by the gadgets. This technique is additionally called Scavenging. since the node is harvesting or collecting unused ambient energy. Energy Harvesting is the most appealing of the three choices because the lifetime of the node would just be restricted by damage or failure of its own parts. In any case, it is possibly the most difficult strategy to use as the energies in different environments differ greatly and exists in several forms and consequently, the solution for every environment and energy form is different. The fundamental test of the nodes is to be self-powering.

Ambient energy can be defined as energy that is not stored explicitly but is available in the device surroundings. These sources have the advantages that they are essentially free; their conversion mechanisms are clean (there is no pollution associated with the conversion process), and the source has a potentially infinite lifespan. Source types and harvesting technologies include solar, thermoelectric, acoustic energy harvesting, the axial-flow micro-turbine generator, and mechanical vibration energy harvesting

2.4. Applications and Market potential

Node-networks have distinct advantages when compared to macro (traditional) sensor networks. On the one hand, traditional sensors are very accurate, but they tend to be bulky and expensive. Due to the high cost, macro sensors are normally implemented in isolation with the effect that the system is not fault tolerant. If one device fails, the system performance is greatly influenced. On the other hand, wireless sensor nodes are relatively low cost. Therefore, the node's sensors are inherently less accurate, but a region can be flooded with multiple nodes. The individual node measurements can be conditioned with advanced DSP's (Digital Signal Processors) to obtain accurate measurements. Furthermore, a network of nodes is inherently fault tolerant as the contribution of each individual node to the total system will be small and a few faulty sensors will not adversely affect the overall system performance. Lastly, a self-powered sensor network has become feasible, as the power requirements of the nodes have decreased.

In certain applications, such as building structural monitoring or environmental control, the node-network will have very long lifetimes. These lifetimes can typically vary from one to 30 years (the typical life of infrastructure). It is desirable to have a node lifetime spanning the application lifetime. Secondly, the size of the complete node should be small enough not to take a lot of space and should be unnoticeable. Potentially, thousands of nodes will be distributed. "Small enough" is application dependent, but most applications desire µm - mm sized devices. Military applications will benefit from a small form factor for these nodes. The I-Bean wireless node (excluding sensor) of dimensions 25 x 15 x 5 mm^3 (volume = 1875 mm^3), which is powered with a Panasonic CR2032 Lithium battery of dimensions; diameter 20 mm, thickness 3.2 mm (volume = 1005 mm^3) has been reported. For this example, the battery constitutes 35% of the total node volume and weighs 3.1 grams.

In terms of cost, the i-Bean wireless sensor node (from Millennial Net) is available for approximately $25, with the goal of a sub-$10 device. If the cost of an individual node is too high, it will not be economically feasible to deploy large networks of these nodes. For the i-Bean nodes, the current power source is a Panasonic CR2032 Lithium battery. The battery cost is around $2.99 - $4.99, so that the battery cost makes up 12 - 20% of the total node price. If the power source can be incorporated into the node, the total cost will decrease. Furthermore, assembly may be eliminated, as there will be no need to install a battery.

Some applications may permanently limit access to the node once it has been deployed. Limited, or no, node access negates the use of power sources with fixed energy densities since operational support (repair and maintenance) for these nodes is impossible. Thus, an infinite power source is desirable. Furthermore, due to the placement and cost constraints on the nodes, it is often not viable to have physical (wired) connections with the nodes, either for communication or power supply. Wiring cost constitutes up to 90% of the total sensor cost in building environment control.

The overall wireless sensors market is estimated to grow to $4 billion by 2020. The worldwide ULP market reached over 200 million units by 2010. Temperature monitoring and vibration spectra of sensitive plant equipment is growing recently around $22m (ARC Advisory Group, 2007). Vibration and velocity sensors and transmitters market are growing from $17.4m in 2006 to $112.5m in 2012 at a compound annual growth rate of 34.4%. In following pie chart, the distribution of wireless sensor nodes in different departments is shown.

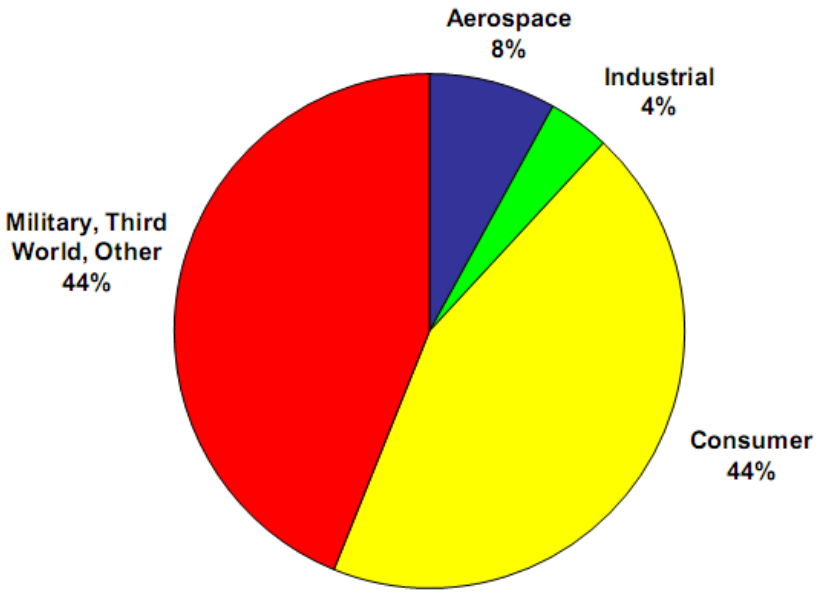

Figure 4 Distribution of Wireless sensor nodes in different markets **(Cottone, 2011)**

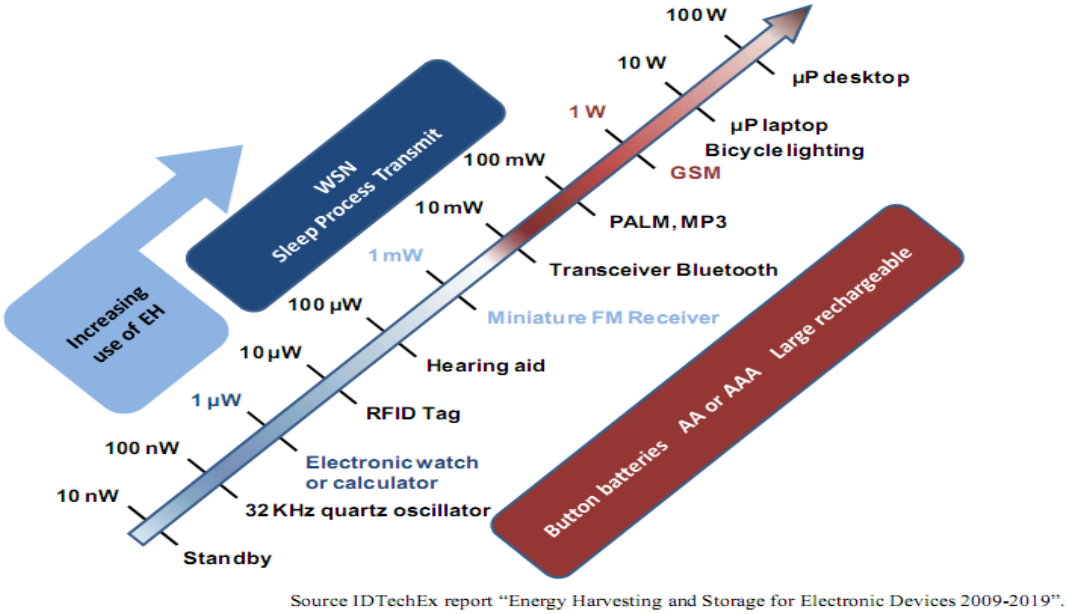

Source IDTechEx report "Energy Harvesting and Storage for Electronic Devices 2009-2019".

Figure 5 Power needs for small electronics **(Cottone, 2011)**

3. Vibration Energy Harvesting

Vibrational energy can be converted to electric energy utilizing one of three mechanisms: the electrostatic, electromagnetic, or piezoelectric effects. These mechanisms will be discussed briefly, before focussing on piezoelectric energy harvesting.

Although conversion of vibrations to electricity is not generally applicable to all environments, it was desired to target commonly occurring vibrations in typical office buildings, manufacturing and assembly plant environments, and homes to maximize the potential applicability of the project. Vibrations from a range of different sources have been measured. A list of the sources measured along with the maximum acceleration magnitude of the vibrations and frequency at which that maximum occurs is shown in Table below. The sources are ordered from greatest acceleration to least.

Vibration Source	Peak Acceleration (m/s^2)	Frequency of Peak (Hz)
Base of 5 HP 3-axis machine tool with 36" bed	10	70
Kitchen lender casing	6.4	121
Clothes dryer	3.5	121
Door frame just after door closes	3	125
Small microwave oven	2.25	121
HVAC vents in office building	0.2-1.5	60
Wooden deck with people walking	1.3	385
Beadmaker	1.03	121
External windows (size 2ft X 3ft) next to a busy street	0.7	100
Notebook computer while CD is being read	0.6	75
Washing Machine	0.5	109
Second story floor of a wood frame office building	0.2	100
Refrigerator	0.1	240

Table 1 List of vibration sources with their maximum acceleration magnitude and frequency of peak acceleration

Additionally, because of interest in embedding self-powered sensors inside automobile tires, acceleration profiles from standard tires have been obtained from the Pirelli tire company (Pirelli, 2002). The "vibrations" exhibited inside tires are significantly different than the other "commonly occurring" sources measured. Therefore, power output estimates and design of devices for this application differ considerably from the standard case.

The three mechanisms are the electrostatic, electromagnetic, and piezoelectric energy conversions. Each mechanism will be discussed next, focusing on applications developed at the small scale.

3.1 Electrostatic Vibration Energy Harvesting

Electrostatic generation consists of two conductors separated by a dielectric (i.e. a capacitor), which move relative to one another. As the conductors move the energy stored in the capacitor changes, thus providing the mechanism for mechanical to electrical energy conversion

This mechanism of conversion is based on the variable capacitor concept. A variable capacitor consists of two conductors separated by a dielectric material. When the conductors are placed in an electric field and the conductors are moved relative to each other, current is generated.

A Simple rectangular parallel plate capacitor can be used to demonstrate the principle of electrostatic energy conversion. The Voltage Across the capacitor is given by the following equation.

$$V = \frac{Qd}{\varepsilon_0 lw} \tag{1}$$

Where

Q is charge on the capacitor

d is the gap or distance between plates

l is the length of the plate

w is the length of the plate

ε_0 is the dielectric constant of free space

The capacitance is given by $C = \varepsilon_0 lw/d$. So, the Current can be given by $i=C*dV/dt$. In the case where charge is held constant, the Voltage can be increased by reducing capacitance which is accomplished by either increasing the gap between the plates or increasing the area of the plates. Similarly, if the voltage is held constant, the charge can be increased by decreasing the distance d between the plates or increasing either one of l or w. In either case the energy stored in capacitor which is given by the equation 2 is increased.

$$E = \frac{1}{2}QV = \frac{1}{2}CV^2 = \frac{1}{2}\frac{Q^2}{2C} \tag{2}$$

The drawback with this method is that a separate voltage source is required to create an electric field because the capacitor must be charged up to an initial voltage for the conversion process to start. Another disadvantage is that for many design configurations mechanical limit stops must be included to ensure that the capacitor electrodes do not come into contact and

short the circuit. The resulting mechanical contact could cause reliability problems as well as increase the amount of mechanical damping. On the other hand, the capacitor configuration is easily integrable into micro-systems using standard MEMS manufacturing processes. Another advantage is that, unlike electromagnetic converters, appropriate voltages for microelectronics, on the order of two to several volts, can be directly generated.

3.2 Electromagnetic vibration Energy harvesting

When a coil is moved within a magnetic field, the current is generated according to Faraday's Law which is given in equation 3.

$$\varepsilon = \frac{-d\phi_B}{dt} \tag{3}$$

Where:

ε is the induced emf

ϕ_B is the magnetic flux

In the simple case of a coil moving through a perpendicular magnetic field of constant strength, the maximum open circuit voltage across the coil is given by equation 4.

$$V_{oc} = NBl\frac{dy}{dt} \tag{4}$$

Where:

N is the number of turns in the coil

B is the strength of the magnetic field

l is the length of one coil (2πr)

y is the distance the coil moves through the magnetic field

A device that employs this type of conversion, is shown in Figure 6.

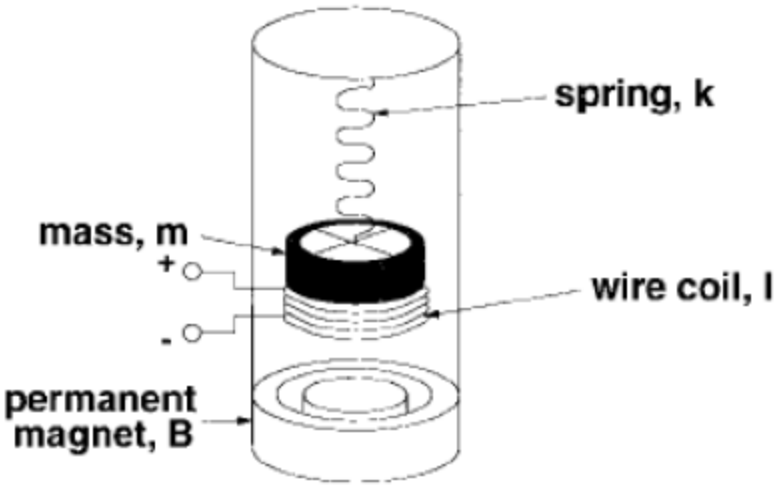

Figure 6 Electromagnetic conversion device

According to (S. Bradai, 2018) Using the baseline vibrations of 2.25 m/s2 at 120 Hz, assuming the maximum device size is $1cm^3$, and making a few assumptions about the strength of the magnetic field and fabrication of the coil, it can easily be shown that maximum output voltage which can be obtained is 0.1V.

This mechanism is utilized to convert vibration into electrical energy and has the following properties:

- No Separate Voltage is required
- A permanent magnetic field is required, Permanent magnets are normally bulky.
- The output voltage is normally around 0.1 - 0.2 V, so it is necessary to transform the voltage to usable levels for nodes.
- well suited for operation at relatively low frequencies in devices of medium size to drive loads of relatively low impedance.
- they are expensive to integrate in microsystems because micro-magnets are complex to manufacture, and relatively large mass displacements are required.

In the following figure the general model of one DOF electromagnetic generator is shown

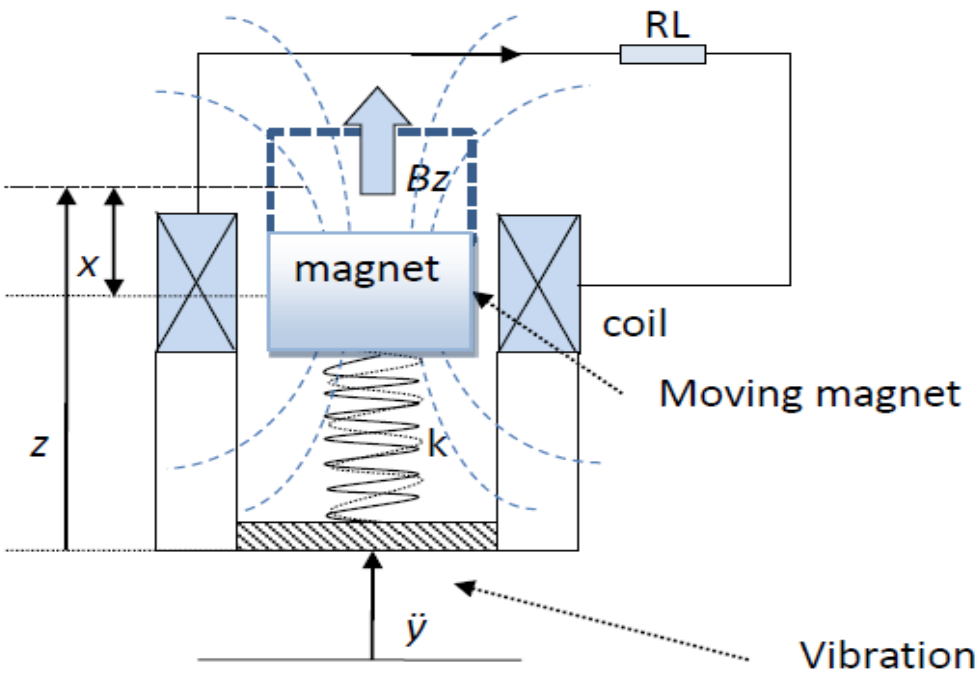

Figure 7 The general model of one DOF electromagnetic generator **(Cottone, 2011)**

The motion equations for simplified one-DOF model of an EM VEH can be written in a general form as following.

$$m\ddot{z} + d\dot{z} + kz = -\alpha V_L - \mathrm{m}\,\ddot{y} \tag{5}$$

$$\dot{V}_L + \omega_c V_L = \delta_c \omega_c \dot{z} \tag{6}$$

Where:

$\alpha = B_z l / R_L$	Electrical coupling force factor
$\delta_c = B_z l$	Conversion factor
$\omega_c = R_L / L_e$	Characteristic cut-off frequency
$L_e = \mu N^2 \pi R^2 / h_b$	Coil self-inductance

For modelling purposes these equations can be converted in Laplace domain and can be processed further to obtain the transfer function and the voltage Frequency response.

$$y = Y_0 e^{i\omega t} \tag{7}$$

The Frequency response of displacement Z and voltage V over input acceleration is given by following expressions.

$$H_{ZY} = \frac{Z}{Y} \tag{9}$$

$$H_{VY} = \frac{V}{Y} \tag{8}$$

The Laplace variable is defined as $\boldsymbol{s = i\omega}$

The equations are written in matrix form by transforming in Laplace domain with s as Laplace variable and solution Z and V are derived from this procedure.

$$\begin{pmatrix} ms^2 + ds + k & \alpha \\ -\delta_c \omega_c s & s + \omega_c \end{pmatrix} \begin{pmatrix} Z \\ V \end{pmatrix} = \begin{pmatrix} -mY \\ 0 \end{pmatrix} \tag{10}$$

$$Z = \frac{-mY(s + \omega_c)}{ms^3 + (m\omega_c + d)s^2 + (k + \alpha\delta_c\omega_c + d\omega_c) + k\omega_c} \tag{11}$$

$$V = \frac{-mY\delta_c\omega_c s}{ms^3 + (m\omega_c + d)s^2 + (k + \alpha\delta_c\omega_c + d\omega_c) + k\omega_c} \tag{12}$$

The electric power P_e across the simple resistive load R_L considering the harmonic input of base $\boldsymbol{y = Y_0 e^{i\omega t}}$ can be given by Ohm's law and is derived as:

$$P_e = \frac{Y_0^2}{2R_L} \left| \frac{m\delta_c\omega_c i\omega}{(\omega_c + i\omega)(-m\omega^2 + di\omega + k) + \alpha\delta_c\omega_c i\omega} \right|^2 \tag{13}$$

The electromagnetic generators are not so well suited for MEMs applications as micro magnets are very complex to manufacture. Also, the electric output pf these generators is low comparatively with other techniques. However, they can be used in medium sized applications that can be used for monitoring. For example, a harvester was developed for the applications in train to be installed in Wagons to monitor certain parameters such as Position and Temperature etc (S. Bradai, 2018).

3.3 Piezoelectric energy Harvesting

This is the most common method used for harvesting energy from vibrations and focus of this thesis. Generally, the model consists of a cantilevered beam with patch of piezoelectric material attached either on both sides of the blade or on one side. Depending on this configuration the harvester can either be unimorph or bimorph. In this process the electricity is generated due to properties of piezoelectric materials. Piezoelectric materials produce electric current when are subjected to mechanical strain energy.

This is the case when the base of a cantilever is exposed to the mechanical vibrations, the cantilever beam produces strain energy which is usually maximum near the base of the cantilever beam and that is where the piezoelectric material is normally coupled with the beam. The maximum power is harvested when the natural frequency of the harvester is matched with the ambient vibrations. That is not normally the case as the vibrations in environment are totally random and have wide spectrum normally. A lot of researchers have proposed the solutions to deal with this problem and for the optimisation of the harvesters.

The most common way of energy harvesting includes the cantilever beam which is covered by one or two layers of piezoelectric patches depending on whether it is a unimorph generator or a bimorph. The beams are attached to vibrating structures and they produce an alternating voltage. In practice this voltage must be converted to constant voltage by using AC-DC rectifier followed by a capacitor, however in mathematical modelling the circuits are simply represented by resistive load. Now a days a lot of research has been also carried out in optimizing the circuits of harvesters which affect greatly the output voltage of a harvester. In beam harvesters at small scale normally there is a need to add a proof mass at the end of a beam, because the natural frequency of the micro beams is very high and in order to reduce the natural frequency the additional mass is added which reduces the first natural frequency of the harvester. Another way of harvesting energy using piezoelectric materials is the direct attachment of piezoelectric patch to the vibrating structures. This technology has several advantages as compared to the beam harvesters as the clamping and the need to add the proof mass is eliminated. It can also harvest energy in wide spectrum more easily than beam harvester because the vibration modes of patch are closely separated as compared to the beam harvester.

3.3.1 Properties of Piezoelectric Materials.

In **1880,** Jacques and Pierre Curie discovered the piezoelectric effect in certain crystalline materials: when these materials are subjected to a mechanical force, their crystals become electrically polarized.Piezoelectric effect is the production of electric current when the mechanical stress is applied and is due to change in polarization of the material. Similarly, these materials also have the inverse piezoelectric affect where, when the electrical energy is applied

to these materials, they undergo the mechanical deformation. The polarities for tensile and compressive forces are opposite in direction. Generally, there is a difference between Piezoelectric and Ferroelectric materials. The materials whose crystals have dipole are piezoelectric materials whereas belonging to this family some materials which can be poled are Ferroelectric materials. It means the direction of the dipole can be changed. These poled materials have strong piezoelectric coupling than their unpoled counterparts and are used in application as sensors and actuators.

Piezoelectric ceramics consist of multiple crystals which are randomly oriented, above certain temperature their geometry changes to cubic and hey no longer exhibit piezoelectric effect. This temperature is called Curie temperature of a Piezoelectric material. However, below this temperature the crystals are elongated and geometry changes to tetragonal lattice and they exhibit dipole moment hence also the piezoelectric effect. The Cubic crystal with no piezoelectric effect and tetragonal crystal with piezoelectric effect are shown in fig 8.

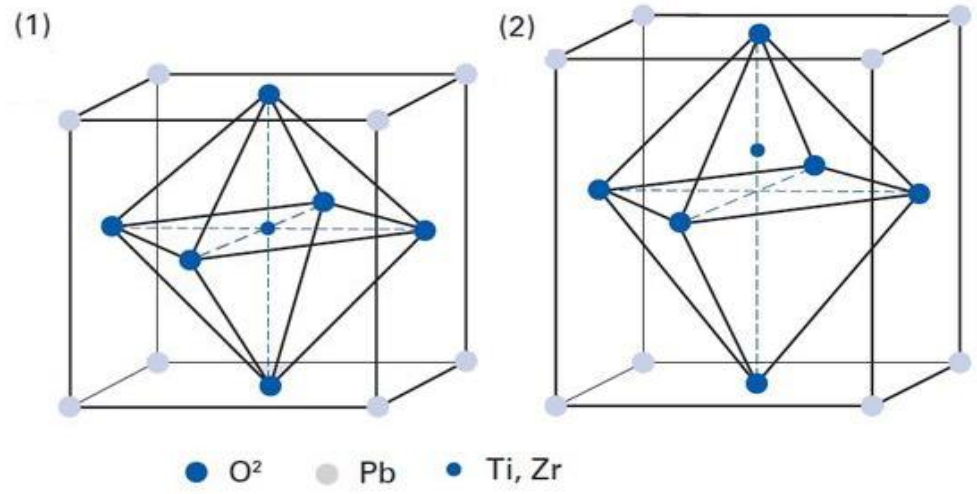

Figure 8 Crystal of PZT above (cubic) and below curie Temperature (tetragonal)

The direction of Polarization is normally totally random in the crystals of ferroelectric materials, so they must be aligned by the process of polarization. The permanent polarization of crystals is obtained by applying a very strong electric field to the crystals just below the curie point. The dipoles which were randomly aligned before are now aligned in the direction of electric field and the material expands in direction of electric field. When the electric field is removed the dipoles stay almost aligned in the direction in which the electric current is applied. This process is used to make the ferroelectric materials with strong piezoelectric coupling. It is also called

the poling of piezoelectric materials. Some ferroelectric materials with high piezoelectric coupling are Lead Zirconate titanate (**PZT**) and Barium Titanate (**$BaTiO_3$**), on the other hand Zinc oxide (**ZnO**) is material with relatively low piezoelectric coupling. the most commonly used Piezo crystals used is Lead Zirconate titanate. The poling scheme of PZT is shown in following figure.

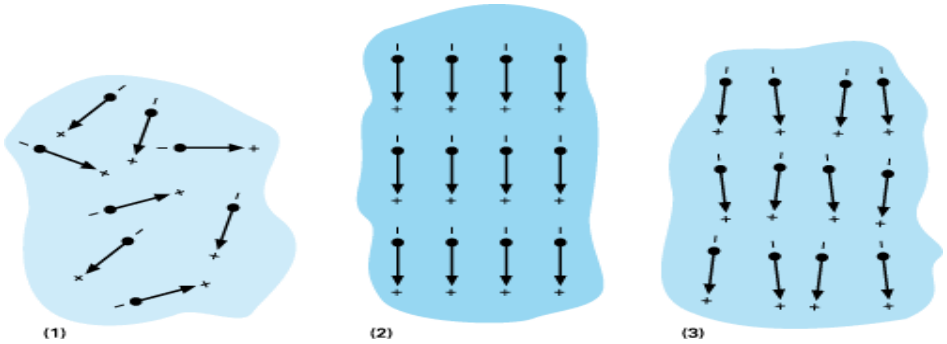

Figure 9 After poling the zirconate-titanate atoms are off center.

In the thin films of piezoelectrics normally the tetragonal layer is aligned with out of plain axis of the film. The dipole direction in the plane is however randomly aligned.

Power density of a generator is defined as the power generated per unit of volume. Power densities of piezoelectric materials are comparable to thin-film and thick-film lithium ion batteries and thermoelectric generators. The voltage output of Piezoelectric generators is higher as compared to electromagnetic generators and can be used to directly charge the capacitors which is not the case in electromagnetic generators where the additional post-processing is required before the final usage. It is also easy to fabricate at small scale applications.

3.3.2 3-3 vs 3-1 mode

Piezo material can be used in 3 ways: the 33 mode, the 31 mode, the 15 mode. The first digit represents the direction in which the voltage is applied, whereas the 2nd digit represents the direction in which the strain is developed. In the 33 mode the voltage along the polarization axis lead to the deformation along the polarization axis whereas in 31 mode if the strain is applied in z direction the voltage is developed in x direction. The 15 mode exists as well but is rarely used, in this case the electrodes must be perpendicular to the 1 axis. This mode uses the shear deformation in 31 plane. Utilising these modes require different types of geometries for each mode. The third axis is normally the thickness direction, the other two directions have larger dimensions than this axis. The 31 mode is applied almost always in the form of a patch. The electrodes are formed on above and below surface of the patch. The patch is then bonded to plate or a beam structure. Applying the bending strain will then produce voltage as direct piezoelectric effect whereas applying voltage will produce strain between the patch.

In past the 33 mode was only utilised by forming the stacks of piezoelectric material as shown in fig 10. The length along 3 direction is typically larger than the cross section of the stack, in recent times however patches have been developed which utilise 33 mode. In practice however 33 mode is not used commonly because it requires the volume of piezoelectric material to be maximum. The stiffness of piezoelectric material is dependent on poling of a material, the stiffness of 31 mode is normally larger than the 33 mode however the difference is not so large. It would suggest that if we consider the power only, the 33 mode of operation is better than 31 mode. The voltage and current developed at the optimum power is dependent on the coupling, hence, material selection particularly the poling plays an important role in designing the harvester. The convention for axis in piezo materials is given in the figure 10.

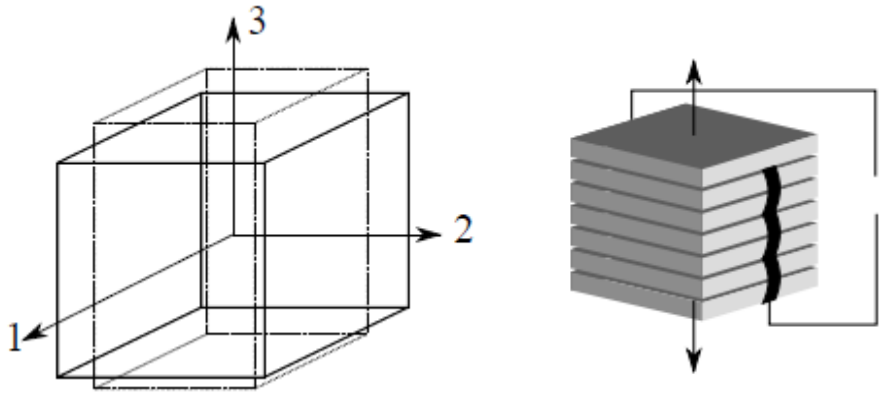

Figure 10(a) Axis notation for Piezoelectric material (polarization in 3) b Stack actuator

One of the advantages of using 33 mode is that voltage can be controlled because for 31 mode electrodes spacing depends on the thickness of a piezoelectric patch and because of relationship between electric field and voltage this electrode spacing determines the voltage developed. The longitudinal (33) piezoelectric effect can be much larger than transverse piezoelectric effect (d33/d31 ~ 2.4 for most piezoceramics). The illustration of 33 and 31 mode is shown in following figure.

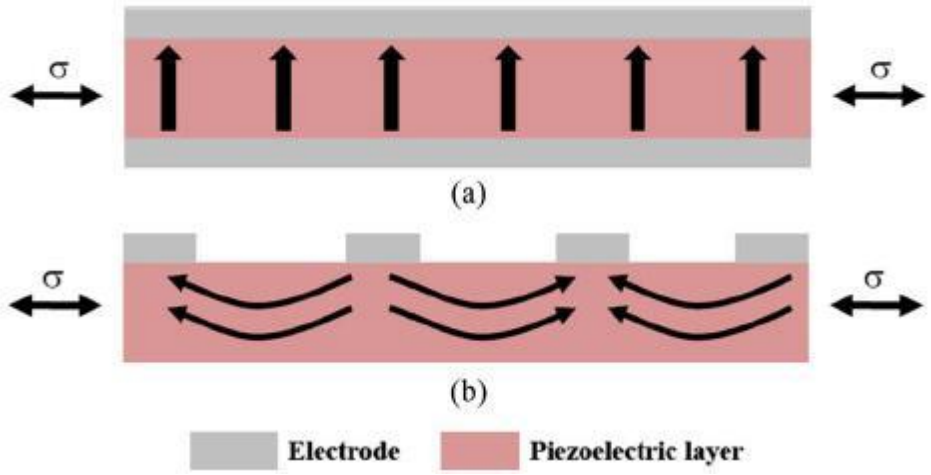

Figure 11 illustration of 31 mode and 33 mode

The longitudinal **{3-3}** piezoelectric effect can be much larger than the transverse **{3-1}** effect *(d33/d 31* ~ 2.4) for most piezoelectric ceramics.

3.3.3 Constitutive equations of Piezoelectric material

Piezoelectric constitutive equations define the interaction between stress (σ), strain (S), charge-density displacement (D), and electric field (E) components of piezoelectric material. Tensorial representation of the constitutive equation can be written as:

$$\sigma = C^E S - e^T E \quad (14)$$

$$D = eS + \varepsilon^S E \quad (15)$$

Variables σ, C^E, S, E, D, e and ε^S represent the stress vector, stiffness matrix, strain vector, voltage field vector [V/m], electric displacement field [C/m^2], piezoelectric coupling matrix in stress charge and permittivity matrix [F/m] at constant mechanical strain. We can see that first part of the first equation is hookes's Law. The stress and strain vectors therefore can be written as:

$$\sigma = \begin{pmatrix} \sigma_{11} \\ \sigma_{22} \\ \sigma_{33} \\ \sigma_{23} \\ \sigma_{31} \\ \sigma_{12} \end{pmatrix} \quad (16)$$

$$S = \begin{pmatrix} S_{11} \\ S_{22} \\ S_{33} \\ 2S_{23} \\ 2S_{31} \\ 2S_{12} \end{pmatrix} \quad (17)$$

The stiffness matrix is a 6x6 matrix which contains elastic stiffness at constant electric field, it is simplified to 6 independent values as in following matrix due to symmetry present in the unit cell.

c11	c12	c13	0	0	0
c12	c11	c13	0	0	0
c13	c13	c33	0	0	0
0	0	0	c44		
0	0	0		c44	
0	0	0			c66

The second part of the 1st equation is stress generated by the piezoelectric effect. It is dependent on the voltage field within the material. Again, considering the atomic structure, simplifications in the number of material parameters are already included. These matrices are then defined as follows

e=

0	0	0	0	e_{15}	0
0	0	0	e_{24}	0	0
e_{31}	e_{32}	e_{33}	0	0	0

$$E = \begin{pmatrix} E_1 \\ E_2 \\ E_3 \end{pmatrix} \quad (18)$$

From the **e** matrix it can be seen that is also possible to impose a shear deformation in the material by applying a voltage along the 1 or 2 axes.

The 2nd equation is an electrical equation. It can be considered equivalent to the mechanical equation with matrices D and E equivalent to strain and stress matrices. The electrical permittivity ε^S is equivalent to mechanical stiffness.

When the material undergoes mechanical strain, the charge is displaced by the piezoelectric and is deposited at the electrodes perpendicular to the 3 axes and in this way the voltage is produced. If we think in terms of mechanical phenomenon it is equal to compressing the spring which requires the force to maintain it. The D and ε matrices are given as:

$$D = \begin{pmatrix} D_1 \\ D_2 \\ D_3 \end{pmatrix} \tag{19}$$

$$\varepsilon^s = \begin{pmatrix} \varepsilon_1 & 0 & 0 \\ 0 & \varepsilon_2 & 0 \\ 0 & 0 & \varepsilon_3 \end{pmatrix} \tag{20}$$

The piezoelectric parameters can be converted from the strain charge to stress charge using following equations.

$$C_E = S_E^{-1} \tag{21}$$
$$e = dS_E^{-1} \tag{22}$$

3.3.4 Equations for Piezo elements

Considering a patch of piezoelectric material operating in 31 mode, and the dimensions along 1, 2 and 3 axes are l, w, t. The young's modulus E_{11} is assumed as 1D stiffness. The axis of interest is 1 in which the length changes. Instead of a voltage field, a voltage V_p is applied. From electrostatics the voltage at a point within a uniform electric field between parallel plates is given by $E = -Vd$, with d the distance from the grounded plate. Since the voltage across the entire material is desired, d is substituted with the thickness of the material t. The dimensionless strain is replaced by the deformation divided by the original length. Lastly, consider an element with a loaded surface area A which is given by wt as we are considering 31 mode. The capacitance is created along 12 surface so the area will be lw. Simplifying the equations 14 and 15 by applying the definition of stress and electric displacement we get the following equations.

$$F = \frac{E_{11} wt \Delta l}{l} + \frac{e_{31} wt V_p}{t} \tag{23}$$

$$Q = \frac{e_{31} lw}{l} \Delta l - \frac{\varepsilon lw}{t} V_p \tag{24}$$

Four parameters are of our interest the piezo displacement Δl, force F, the voltage V_p and the current as we are dealing with energy harvesting which is given by time derivative of Q. ***I=dQ/dt.*** The above equations can be modified as:

$$F = \frac{E_{11} wt}{l} \Delta l + e_{31} w V_p \tag{25}$$

$$I = e_{31} w \dot{\Delta} l - \frac{\varepsilon lw}{t} \dot{V_p} \tag{26}$$

Equations 23 and 24 shows a number of meaningful quantities regarding energy harvesting. The mechanical stiffness which is $\boldsymbol{k_p = \frac{E_{11} wt}{l}}$**.** Capacitance of the piezo element which is given by $\boldsymbol{C_p = \frac{\varepsilon lw}{t}}$**.** It is defined in the terms of permittivity. The electromechanical coupling constant $\boldsymbol{\vartheta = e_{31} w}$**.** It links applied voltage to the piezoelectric generated force. The following simplified equations are written for piezoelectric element.

$$F = k_p z + \vartheta V_p \tag{27}$$

$$I = \vartheta \dot{z} - C_p V_p \tag{28}$$

Where z is the displacement and is put in the place of elongation.

When Piezo is used as an actuator a voltage is applied to the piezo element and the strain is produced so only the equation 25 remains whereas when it is used as a sensor a very high resistance is attached to the electrodes of the piezo element thus specifying the open circuit conditions. So, the current flow becomes zero because of the sufficiently large resistance. The left-hand side of the equation 26 becomes zero.

The power is dissipated in the resistor connected along the electrodes because there is current flowing through it as well as voltage present. From Ohm's law we know that P=VI. Power is only produced when the velocity as well as force is present. If a resistor of finite value is connected along the electrodes, the relation V=IR holds and the equation 26 can be rewritten as:

$$\frac{V}{R} = \vartheta \dot{z} - C_p V_p \tag{29}$$

This is the most basic equation used for energy harvesting in which the AC current can be obtained if only the resistor is used as the circuit.

3.4 1D electromechanically coupled model

In this model a simple spring mass damper vibrating system is considered with the piezoelectric bulk in 33 mode inside. The damping term has two terms in this problem, the mechanical damping and the electrical damping. It can be further divided in two categories, the direct force generator and the inertial force generators, the inertial force generators are more flexible as compared to the direct force generators because they require only one point of attachment to the moving structure. The scheme of a generic single degree of freedom generator is shown in the figure 12.

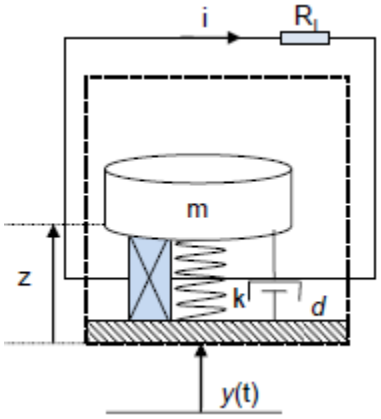

Figure 12 Model of 1d dynamic system with piezo element

Here y(t)is the displacement of the base, z is the deflection of the spring and relative displacement with respect to the frame of reference, m is the mass, a spring of stiffness k and d as mentioned earlier the damping coefficient. d consists of mechanical and electrical damping term; the mechanical damping term depends on several factors but mainly the velocity of the vibrating system the air damping acts on the absolute velocity of the system whereas, strain rate damping acts on the relative velocity of the beam, whereas transduction mechanism induces the additional damping in the system due to conversion of mechanical energy into electrical energy. By looking at the equilibrium of the system the equations of motion of this electromechanical system can be written as.

$$M\ddot{z} + D\dot{z} + Kz + \vartheta V_p = -M\ddot{y} \tag{30}$$

$$\frac{V}{R} = \vartheta\dot{z} - C_p V_p \tag{31}$$

The equation 30 without the coupling term θV_p is just the equation of motion of the simple spring mass system. The high electromechanical coupling term affects the mechanics of the system with the generated electrical energy. The harvested energy diminishes the structural vibrations during harvesting of the energy and consequently the harvested energy is reduced as

well. Considering the harmonic input to the system $y=Y_0e^{j\omega t}$, $z=Z_0e^{j\omega t}$ the equation becomes. If we divide the equation 30 by total mass M, we can find a few important parameters.

$$\ddot{z} + 2\xi\omega_n\dot{z} + \omega_n^2 z + \frac{\vartheta}{M}V_p = -\ddot{y} \tag{32}$$

Considering the harmonic input and performing some normalizations to find the dimensionless constants the equations for frequency response for relative displacement z, Voltage and Electrical power can be found which are given by the following equations.

$$\left|\frac{z}{M\ddot{y}}\right| = \frac{1}{K}\frac{\sqrt{1+(\alpha\Omega)^2}}{\sqrt{[1-(1+2\xi\alpha)\Omega^2]^2+[\Omega\left(2\xi+\alpha\left(1+k_e^2\right)-\alpha\Omega^3\right]^2}} \tag{33}$$

$$\left|\frac{V}{M\ddot{y}}\right| = \frac{1}{|\vartheta|}\frac{\alpha k_e^2\Omega}{\sqrt{[1-(1\ +\ 2\xi\alpha)\Omega^2]^2+[\Omega(2\xi+\alpha(1+k_e^2)-\alpha\Omega^3]^2}} \tag{34}$$

$$\left|\frac{P}{(M\ddot{y})^2}\right| = \frac{\omega_n}{K}\frac{\alpha k_e^2\Omega}{[1-(1\ +\ 2\xi\alpha)\Omega^2]^2+[\Omega(2\xi+\alpha(1+k_e^2)-\alpha\Omega^3]^2} \tag{35}$$

The maximum power that can be achieved by the harvester is at resonance frequency so the equation for maximum power can be simplified by setting frequency of excitation equal to the resonance frequency of the system. And the expression can be defined as:

In the above conditions the ω_n is the fundamental natural frequency of the system and is given by $\omega_n^2 = K/M$, the damping ratio is given by $D=2M\xi\omega_n$, Ω is a dimensionless parameter which is given by $\Omega = \omega/\omega_n$ and dimensionless electromechanical coupling factor is given by

$$k_e^2 = \frac{k_p^2}{1-k_p^2} \tag{36}$$

This constant related the produced electric power to the input mechanical power and vice versa, $\boldsymbol{k_e^2}$ is a critical value which is a measure for the mutual influence of the electrical domain on the mechanical domain. It is the driving factor behind the coupled behavior of electromechanical systems. And the dimensionless time constant $\alpha=\omega_n RC$ where RC is the time constant of the electrical circuit and $1/\omega_n$ is related to the mechanical system .

Normally the harvester is examined at two extremes i.e. R=0, and R= ∞, and the Natural frequency is different at short circuit conditions and open circuit conditions which has also been referred to the antiresonance frequency of the system in the literature. In the first case all the terms with coupling term ϑ vanish and we have the 2nd order equation of mass spring system, whereas in 2nd case the stiffness term is reduced to ϑ^2/C_p and the damping term vanishes and the expressions for the natural frequencies are recorded as:

$$\omega_{s.c} = \sqrt{\frac{K}{M}} \tag{37}$$

$$\omega_{o.c} = \sqrt{\frac{K + \frac{\vartheta^2}{C_P}}{M}} \tag{38}$$

These two equations show clearly the change in dynamic systems due to the effect of piezoelectric coupling, the change in stiffness due to the coupling effect cause the shift in natural frequency in case of the open circuit system in this SDOF modeling method, the similar change in continuous systems can also be expected. The open circuit frequency can be normalized with the short circuit frequency, which is normally purely mechanical domain, using k_{33}^2:

$$\frac{\omega_{0.c}}{\omega_{s.c}} = \sqrt{1 + k_e^2} \tag{39}$$

The Electric equations used for the electrical output in harvester devices directly connected to a resistor are:

$$V = IR \tag{40}$$

$$P = VI \tag{41}$$

Where V represents the voltage across the resistor, I shows the current across the resistor and P shows the power which is dissipated in the resistor which can relate to the power which is being produced by the device.

The analysis is performed on single degree of freedom system with the following parameters assumed.

Mass(Kg)	c_s(Nsm^{-1})	ω_n	K_e	K(Nm^{-1})	Θ(NV)	C_p	Acceleration(ms^{-2})
0.007	0.05	117.31	0.5	4150	-0.0047	2.9 x 10^{-8}	10

The voltage at open and short circuit conditions in a SDOF is calculated, the open circuit conditions is supposed by selecting a very high resistance value and the voltage at short circuit

conditions is calculated by selecting a very low value of resistance, The voltage frequency response with respect to the frequency ratio is calculated by using equation 34 is shown in following figures as well as the maximum voltage at the resonance is compared for different resistances for a given system.

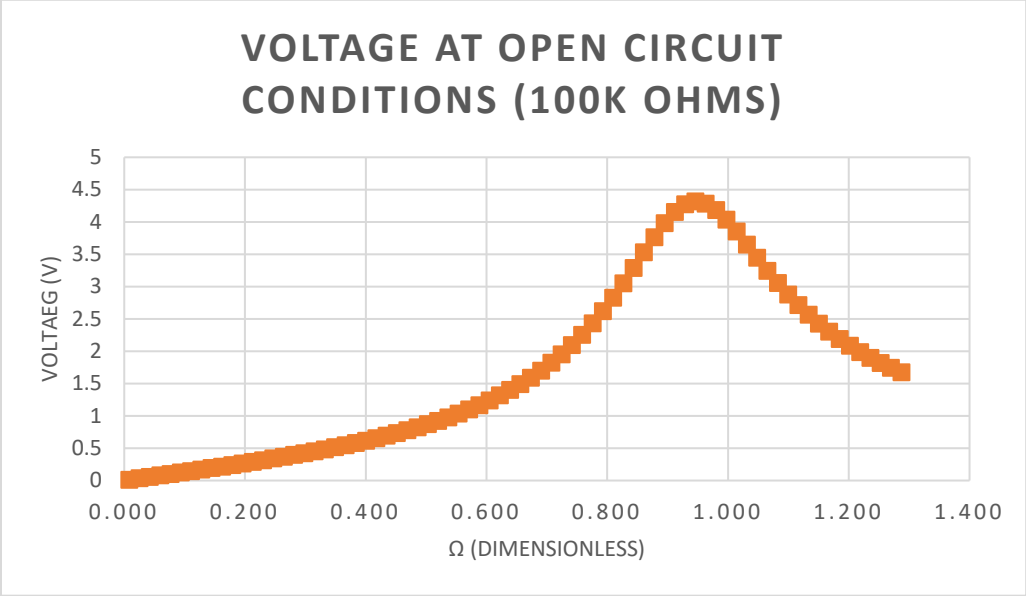

Figure 13 Voltage output at open circuit conditions

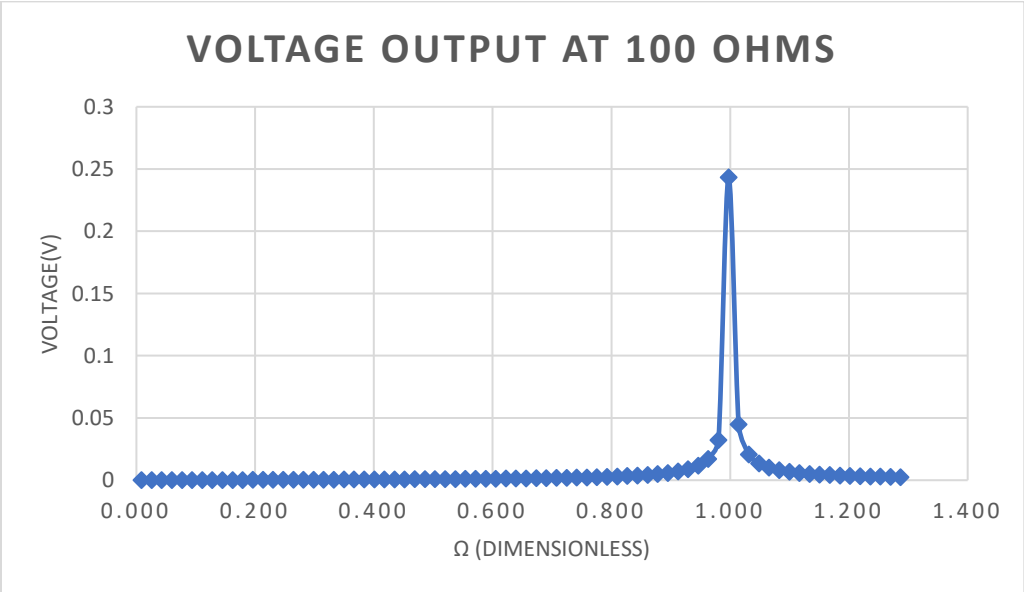

Figure 14 Voltage output at 100 ohms

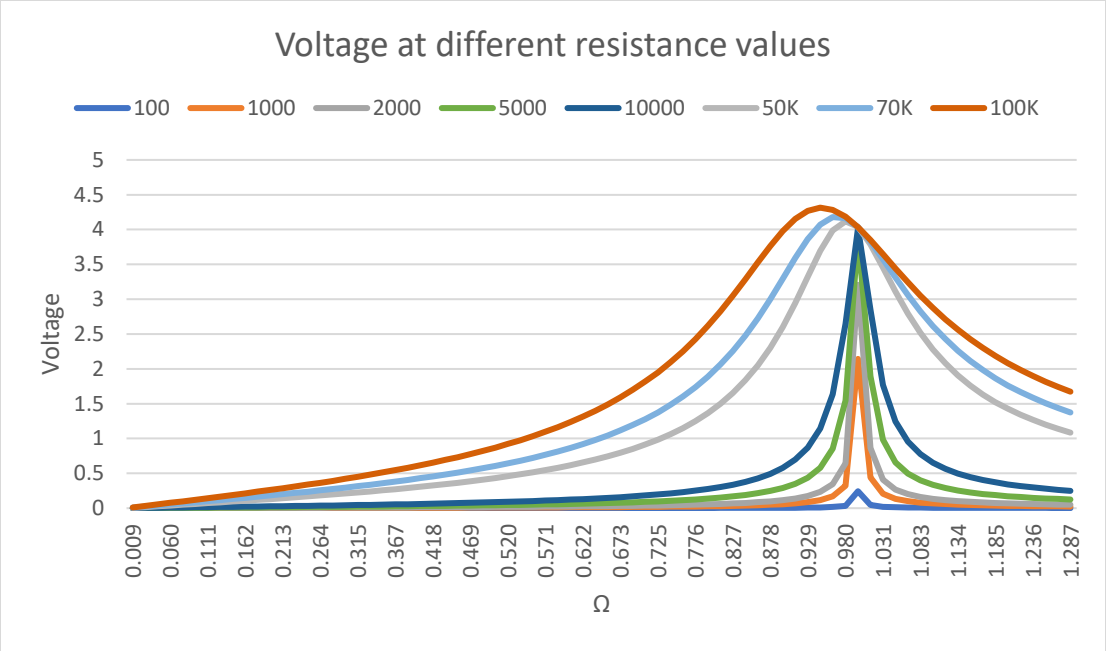

Figure 15 Voltage at different values of resistances

It is noted that the voltage at small resistance values is small and as the resistance value is increased the voltage starts to build up at the resonance frequencies, furthermore, the voltage peak at very high resistance value is shifted to the left. In the following figure the comparison of maximum voltages obtained at resonance frequencies at different resistance values is shown. It can be noted that after a certain value of resistance the voltage is almost constant or at the very high resistances it starts to drop a little. It is seen that after a certain resistance value which in this case is around 10K ohms the Voltage remains constant, so the open circuit condition is achieved

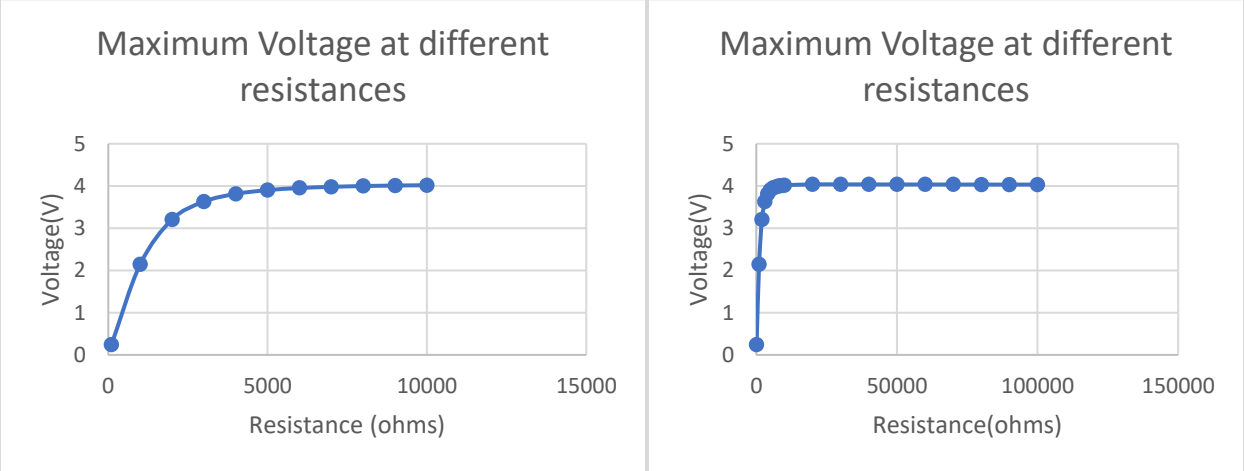

Figure 16 Voltage at resonance with respect to different resistors

In the case of power there is an optimal value of resistance at which the maximum power can be extracted. This procedure of finding the optimal resistance is called impedance matching. Some results of power output are shown in following figures.

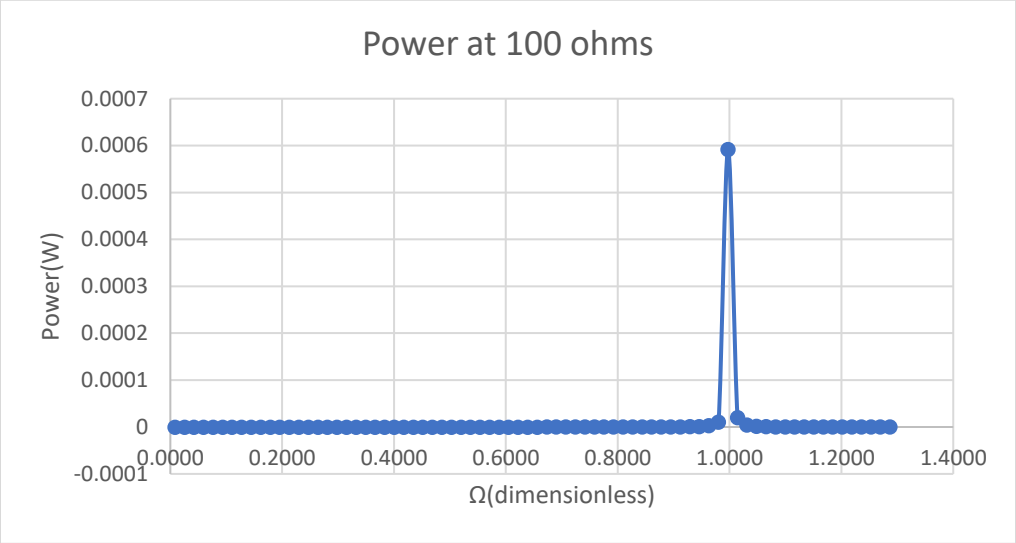

Figure 17 Power output at short circuit conditions

The power output at 100 ohms which is considered as a short circuit condition has a very sharp peak at resonance whereas the power output at 100K ohms(open circuit conditions) is relatively smooth. One of the problem while energy harvesting is exciting a structure at very narrow range of frequency because the power is available only around the resonance frequency, especially in the structures whose damping coefficient is low.

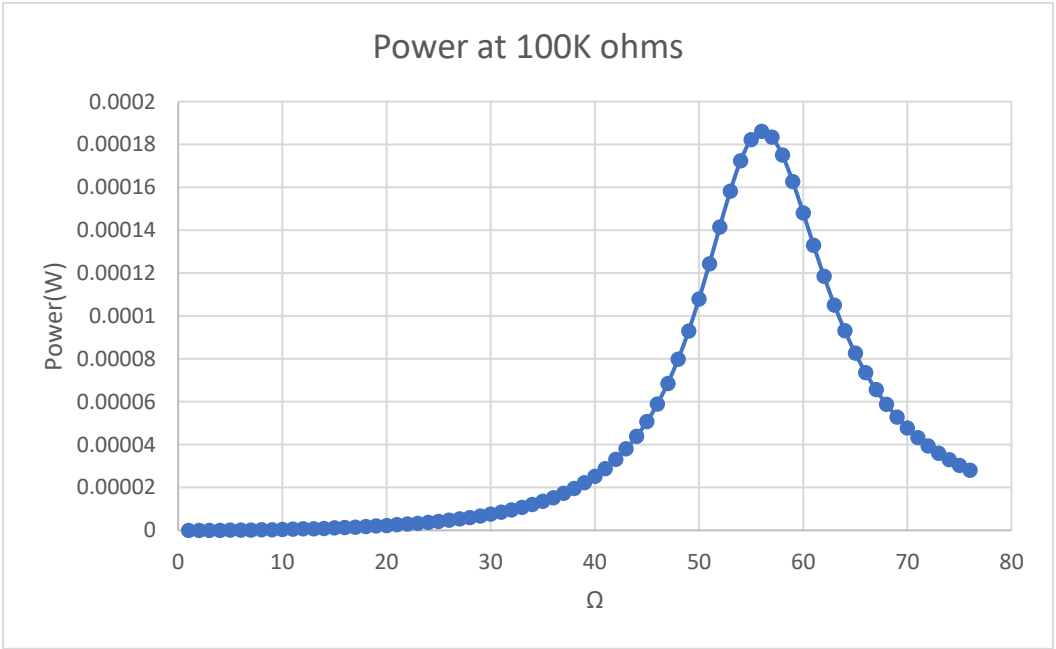

Figure 18 Power output at open circuit conditions

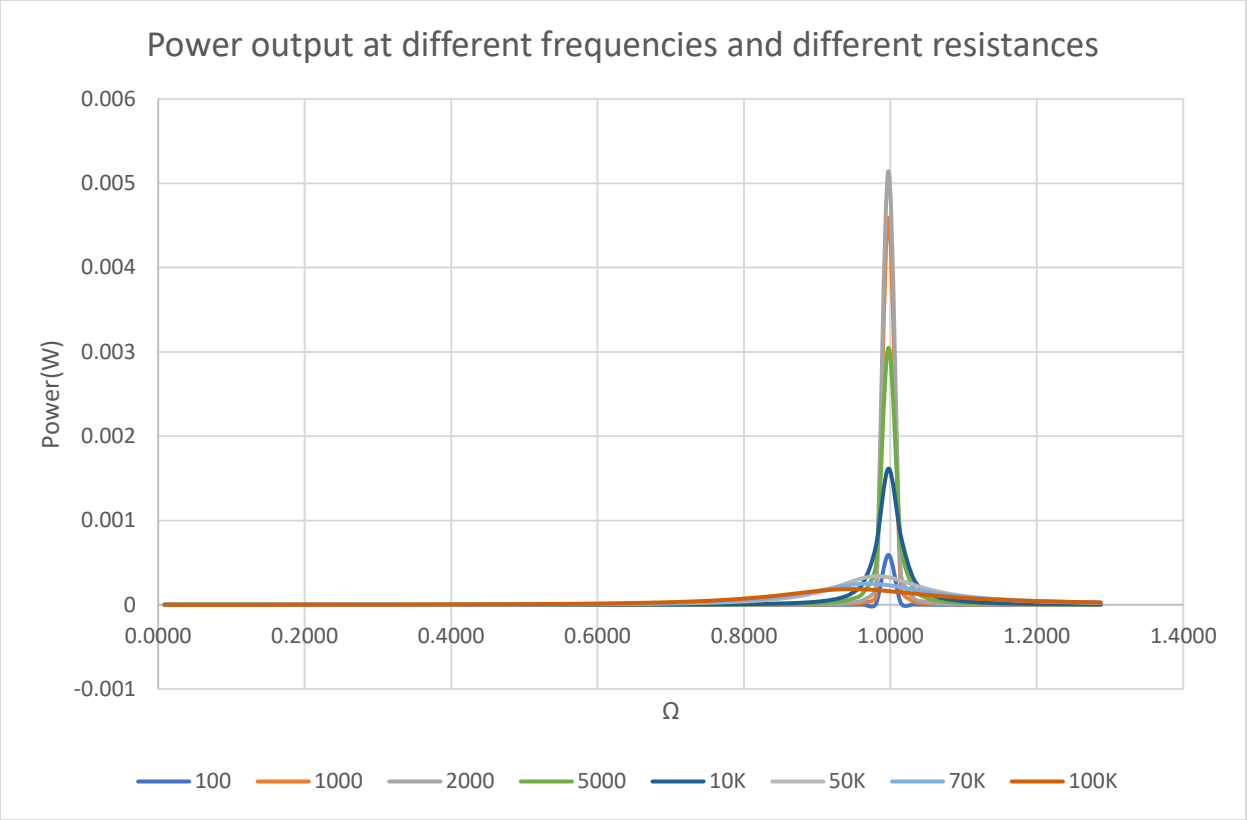

Figure 19 Power output at different resistance values

The maximum power available at resonance differs for different values of resistances and there exists the optimal value of resistance at which the power dissipated in resistor is maximum and should be selected in the electrical circuit. This procedure is called Alternate Current impedance Matching (ACIM) as there is no rectifier or diode bridges considered in this analysis to convert the alternating voltage into the Direct voltage. The maximum power available from the structure is shown in accompanying graph.

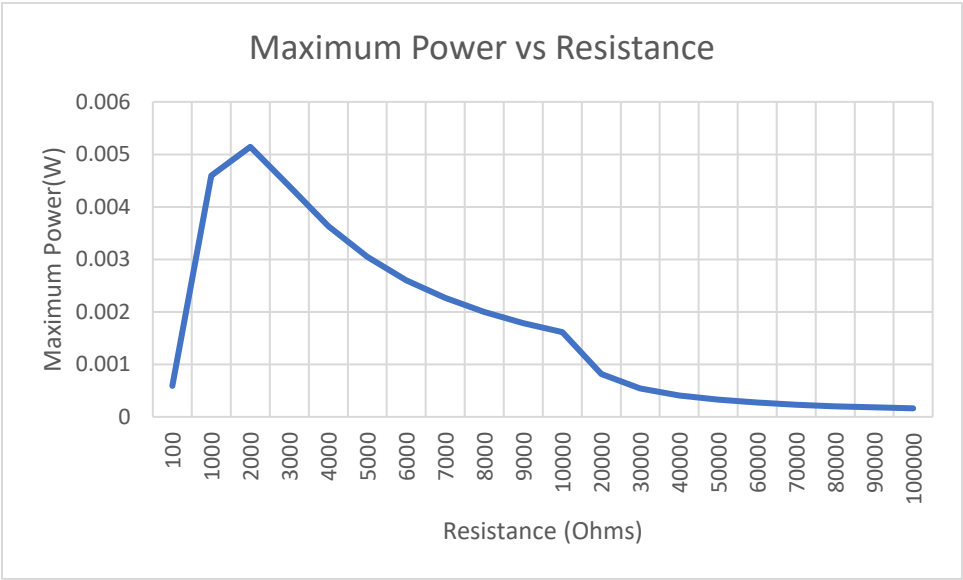

Figure 20 Maximum Power vs Resistance

It is quite clear from the above graphs that the maximum power available for the given system is harvested at 2000 ohms resistor, So this is the best value for the resistance to choose in this case, It is different in different systems depending on the electrical and mechanical parameters of the system.

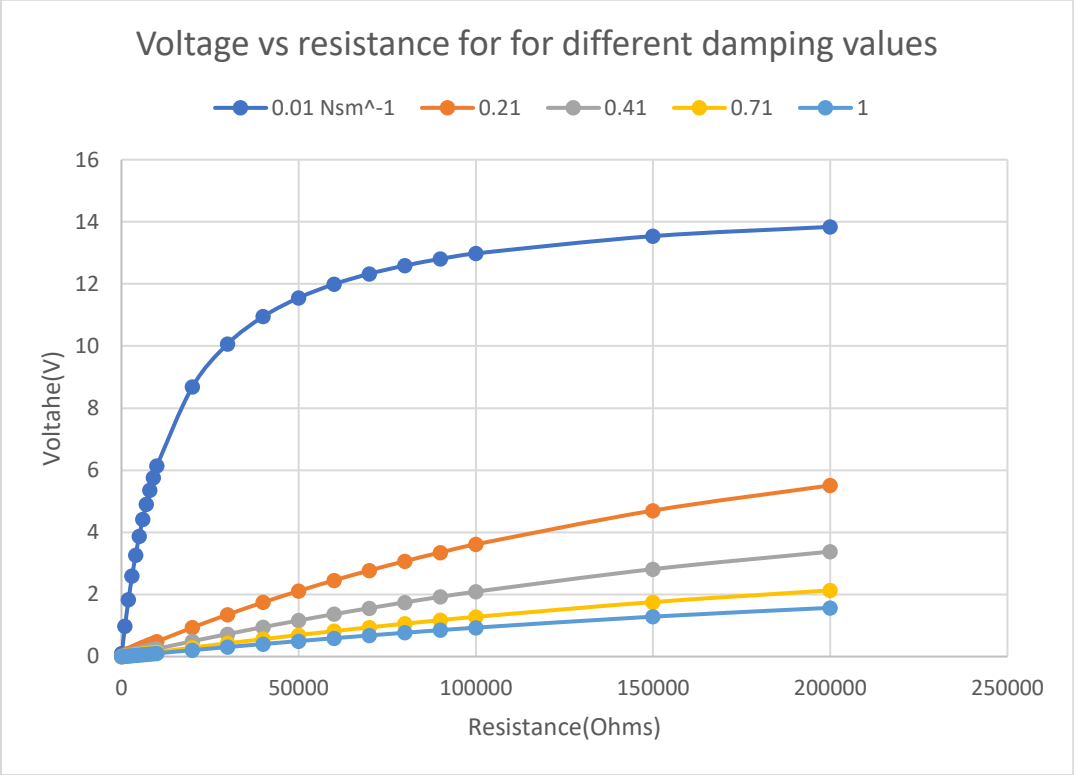

Figure 21 Maximum voltage at different resistance values for different damping values

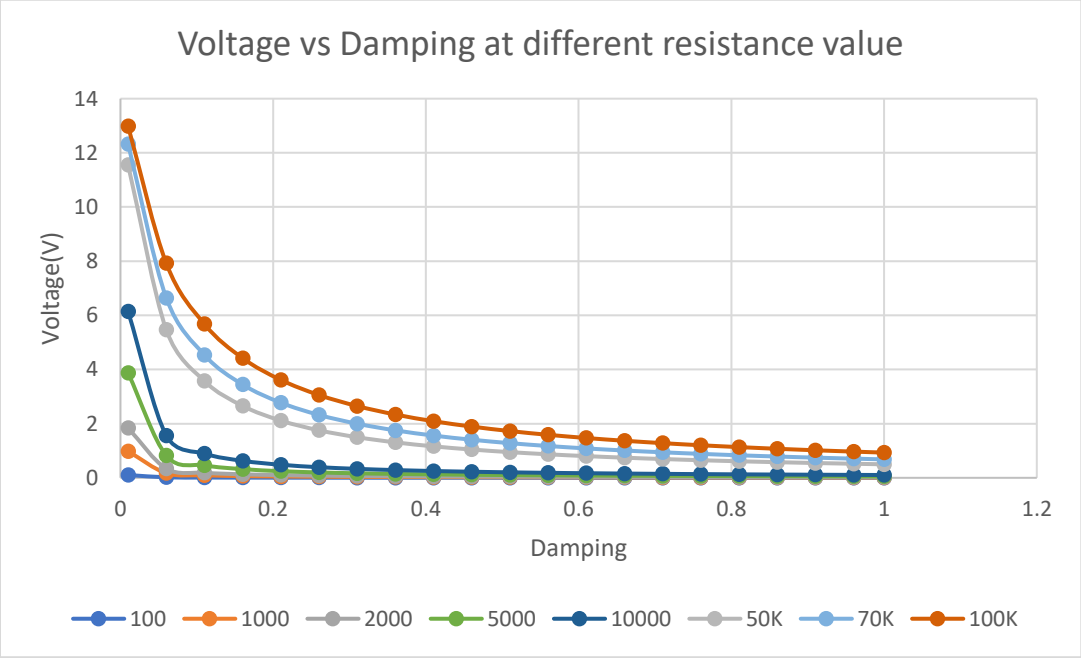

Figure 22 Maximum voltage at different damping values for different resistances

3.5 Distributed Parameter Model of Electromechanically Coupled Cantilever beam

Erturk and Inman (A. Eturk, 2008) studied the distributed model of the cantilevered beam which studies the Piezoelectric energy harvesters with continuous systems approach. The SDOF demonstrating approach or the lumped parameter modeling considers the cantilevered as a mass-spring damper framework, which is helpful for coupling the mechanical some portion of the harvester with a basic electrical gathering circuit. In spite of the fact that SDOF demonstrating gives beginning knowledge into the issue by permitting basic shut structure articulations, it is only a basic estimate constrained to a solitary vibration mode of the beam and it comes up short on a few significant parts of the physical framework, for example, the dynamic mode shape and the precise strain distribution along the bender. When a structure is excited by the motion of its base, the excitation source is nothing but its own inertia. So, the conventional approach of the SDOF results in underestimation of the response especially if there is no tip mass attached.

They used the Euler-Bernoulli Beam assumptions and the more advanced damping mechanisms (i.e. considering internal strain rate damping and external air damping mechanisms) derived the equations for exact solution of electromechanically coupled piezoelectric energy harvester for transverse vibrations. The model they used in their analysis is shown in accompanying figure.

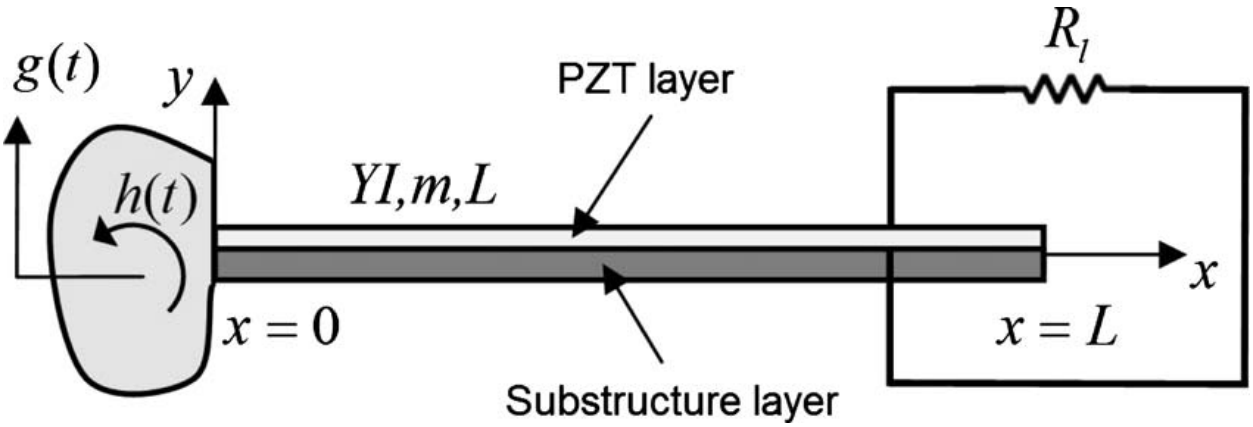

Figure 23 Piezoelectric Energy Harvester under translational and small Rotational base motion (A. Eturk, 2008)

The differential equation governing the mechanical movement of the host plate and the piezoceramic fix with electrical coupling can be expressed as

$$D\left(\frac{\partial^4 w(x,t)}{\partial x^4}\right) + c_s I \frac{\partial^5 w(x,t)}{\partial x^4 \partial t} + c_a \frac{\partial w(x,t)}{\partial t} + m\frac{\partial^2 w(x,t)}{\partial t^2} + \vartheta V(t)\left\{\left[\frac{d\delta(x)}{dx} - \frac{d\delta(x-L)}{dx}\right]\right\} = -m\frac{\partial^2 w_b(x,t)}{\partial t^2} - c_a \frac{\partial w_b(x,t)}{\partial t} \quad (42)$$

where *w*(*x*, *t*) is transverse deflection of the plate at relative to its base and at time *t* . $c_s I$ is the equivalent damping term of the composite cross section due to structural viscoelasticity (c_s is the equivalent coefficient of strain rate damping and *I* is the equivalent area moment of inertia of the composite cross section), c_a is the viscous air damping coefficient, and *m* is the mass per unit length of the beam. Both of the damping mechanisms considered in the model satisfy the proportional damping criterion, hence, they are mathematically convenient for the modal analysis solution procedure, w_b is the displacement of the base of the beam. This equation can be solved to get the expression of voltage across the resistive load at arbitrary frequency as a response to the base acceleration of the beam. Which can be further reduced around the resonance frequency as the maximum voltage is produced at the resonance frequency. Assuming the harmonic motion of the base and ω as the excitation frequency, the voltage response is derived as:

$$v(t) = \frac{\sum_{r=1}^{\infty} \frac{jm\omega^3 \varphi_r \gamma_r^w}{\omega_r^2 - \omega^2 + 2j\xi\omega_r\omega}}{\sum_{r=1}^{\infty} \frac{j\omega X_r \varphi_r}{\omega_r^2 - \omega^2 + 2j\xi\omega_r\omega} + \frac{1 + j\omega\tau_c}{\tau_c}} \quad (43)$$

The voltage around the fundamental natural frequency is reduced as following:

$$v^*(t) = \frac{jm\omega^3 \varphi_1 \tau_c \gamma_1^w}{j\omega X_1 \varphi_1 \tau_c + (1 + j\omega\tau_c)(\omega_r^2 - \omega^2 + 2j\xi\omega_r\omega)} \quad (44)$$

Once the time history of voltage is obtained the current generated by the harvester can be calculated by the relation V=IR and instantaneous power can be computed by Ohm's law

4. Finite element Model

To Conduct the Finite element analysis Ansys FEM software was used. The Cad model I chose to work on is given in the following figure. The cad model is developed in the software DesignModeler which is a built in Cad software for Ansys.

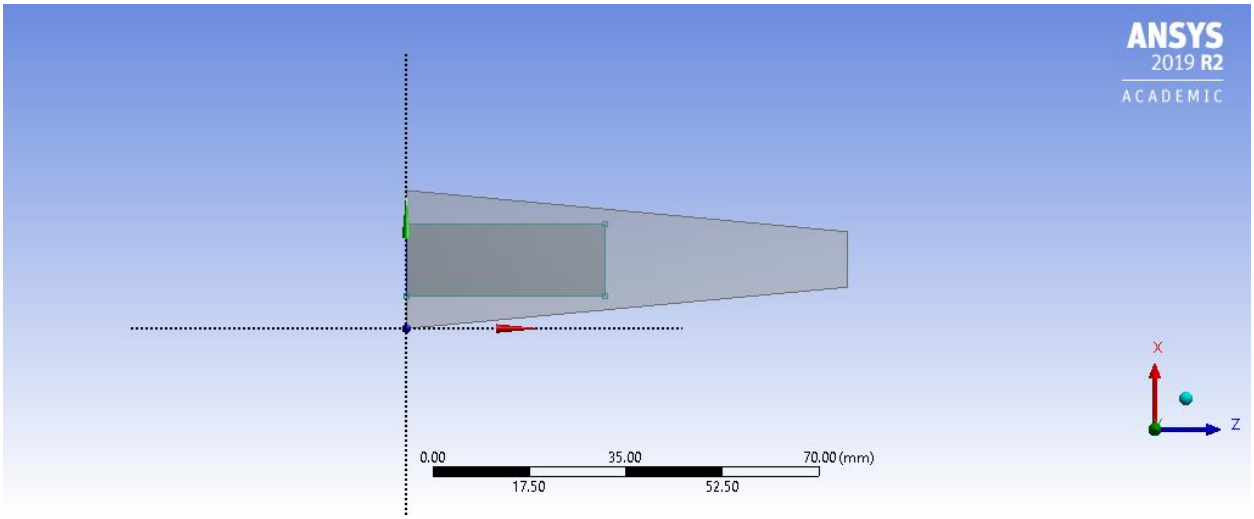

Figure 24 Cad model of the trapezoidal cantilever beam.

The chosen material of the cantilever beam is structural steel which is present in the catalogue of the Ansys 19.1 and the dimensions and the physical properties of the cantilever are given in the table below.

Material	Structural steel
Length	250 mm
Width	Trapezoidal (44-25) mm
thickness	0.8 mm
Fundamental Natural frequency	117.31
damping	0.01
Density	7850 kgm^-3

4.1 Optimal shape

The trapezoidal shape is chosen for the beam because according to previous research the over strain occurs in the rectangular beams. Electrical energy output is proportional to mechanical strain applied. So, to fully utilize the potential energy in piezoelectric material to maximize the strain at each point in the beam is a priority. Ideally, when the beam is deformed the strain distribution in the beam would be completely uniform and at the strain limit. But it can be seen that in the practical cases the stress concentration is maximum at the base and near the clamped end of the beam, this is mainly due to the moment induced by the mass. There exists a small area of maximum strain near the base of the cantilever, whereas near the tip there is hardly any strain at all. As we know that the electrical energy is extracted from the strain energy of the beam so if the beam is fully covered with the piezo element almost half of the piezo element will be unused. It has been seen that this problem can be solved by modifying the shape of beam to trapezoidal or the triangular shape. It allows a more uniform strain distribution and the average strain can be raised significantly, relatively reducing this problem. The strain energy analysis was performed in Ansys workbench to look for this problem in a rectangular beam and the result is shown in the following figure.

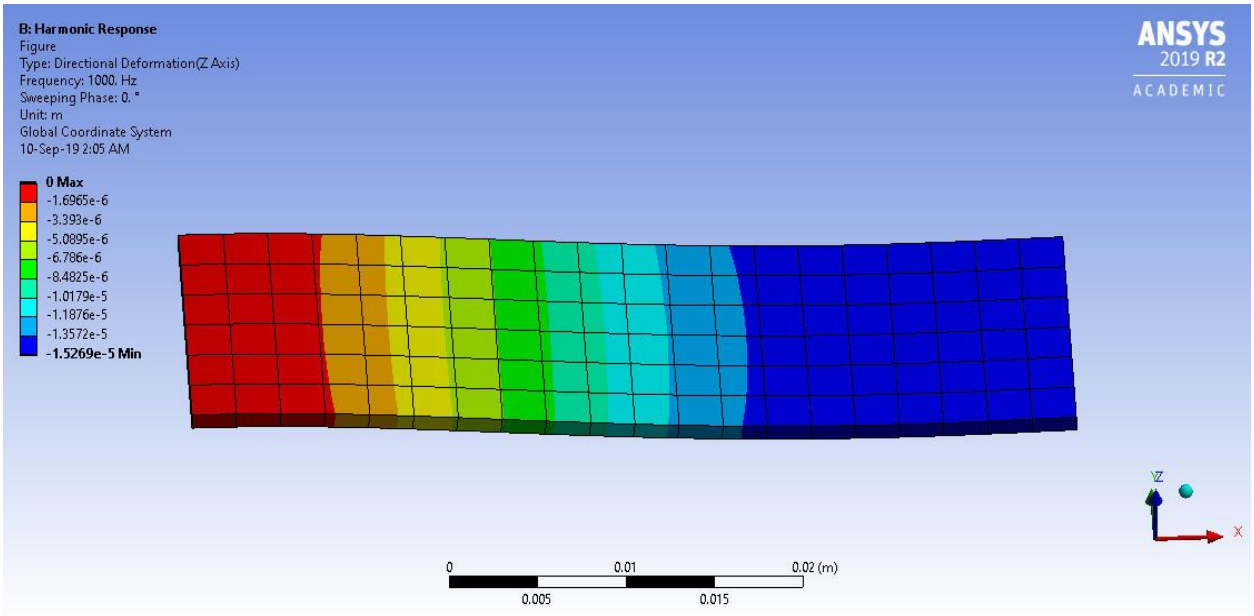

Figure 25 Deformation of a rectangular beam.

It can be seen in this figure that the maximum strain at all is near the clamped end of the beam and towards the tip there is no strain at all. This is quite a non-uniform behavior, so the shape chose for this project was Trapezoidal.

4.2 Piezoelectric Element

The piezoelectric element selected for this project is Lead zirconate Titanate from Fuji Ceramics corporation Japan. The category of the material is C-6 and the list of properties are shown in the figure 14 which is taken from the official website of the Fuji ceramics corporation. (Products by Digital book, 2018).

The piezoelectric parameters can be converted from the strain charge to stress charge using following equations.

$$C_E = S_E^{-1} \quad (23)$$

$$e = dS_E^{-1} \quad (24)$$

The physical dimensions and further properties of the Piezo element are given in following table.

Piezoelectric actuator	Lead Zirconate Titanate C-6
Length	80.17 mm
Width	24.959 mm
thickness	0.3 mm
Density	7650 kgm^-3
e33	-3.85
e31	8.42
e15	14.4

The material characteristics of piezoceramics

• PZT–$Pb(Zr{\cdot}Ti)O_3$／The lead zirconate titanate materials (soft ceramics).

Material No.			C-5	C-6	C-6H	C-62	C-63	C-64	C-601	C-7	C-8
Use exampls.			Bone MICs, Sonic sensors	Transmit-receive sensors of ultrasonic (for cars, flowmeters, bubble sensors & level meters, etc.), Ultrasonic medical probes (for diagnostic imaging), for various actuators						Sound pickups	
Coupling factors.	$\times10^{-2}$	k_p	64	66	70	68	59	63	65	58	65
		k_{31}	38	39	41	40	33	35	37	34	38
		k_{33}	73	76	77	77	68	73	76	72	77
		k_t	53	52	50	52	48	50	50	53	52
		k_{15}	78	74	76	76	66	71	73	64	70
Frequency constants.	m・Hz	N_p	2060	1960	1960	1960	2130	1970	2060	2080	1980
		N_{31}	1530	1420	1420	1440	1480	1380	1460	1440	1410
		N_{33}	1400	1350	1380	1350	1500	1360	1380	1410	1350
		N_t	2050	2010	2110	2040	2060	1970	2070	2070	2050
		N_{15}	850	850	860	850	950	850	890	950	910
Dielectric constants.		$\varepsilon_{11}^T/\varepsilon_0$	2140	2270	2550	2730	1850	1960	2400	3670	3100
		$\varepsilon_{33}^T/\varepsilon_0$	1170	2130	2400	2600	2000	1850	2300	4660	3480
Piezoelectric charge constants.	$\times10^{-12}$ m/V(C/N)	d_{31}	-140	-210	-240	-234	-165	-185	-210	-271	-274
		d_{33}	333	472	490	500	320	435	500	665	627
		d_{15}	764	758	800	860	530	670	730	737	779
Piezoelectric voltage constants.	$\times10^{-3}$ V・m/N(m^2/C)	g_{31}	-14.5	-11.5	-11.2	-10.6	-9.5	-11.4	-10.0	-6.8	-8.8
		g_{33}	32.1	25.0	23.2	24.4	23.0	24.4	23.0	15.0	19.7
		g_{15}	40.3	37.7	35.6	35.6	32.5	38.5	34.0	22.7	28.4
Yungs mdulus.	$\times10^{10}$ N/m^2	$Y_{11}^E=1/s_{11}^E$	7.2	6.2	6.3	6.3	6.7	5.9	6.7	6.1	6.0
		$Y_{33}^E=1/s_{33}^E$	5.3	4.9	5.2	4.9	6.2	5.1	5.0	5.2	4.8
		$Y_{55}^E=1/s_{55}^E$	1.9	1.9	2.0	1.9	2.5	2.0	2.2	2.4	2.2
Poisson's ratio.		σ	0.29	0.32	0.31	0.30	0.37	0.34	0.33	0.39	0.32
Mechanical Q		Qm	90	80	70	75	90	80	110	45	65
Dissipation factor.	%	$\tan\delta$	1.65	1.60	2.0	1.65	1.2	1.5	0.9	2.50	1.90
Curie point.	℃	Tc	305	295	290	245	295	345	285	162	193
Density.	$\times10^3$ kg/m^3	ρ	7.65	7.65	7.8	7.60	7.6	7.7	7.8	7.40	7.45
Temp. coefficient.	f_rTC ppm/℃	-40～+20℃	-550	-330	-250	-380	-20	-180	-260	-540	-340
		+20～+80℃	-680	-130	-5	170	80	180	-120	180	-20
	CTC ppm/℃	-40～+20℃	4230	3590	3400	3860	1850	3500	3300	4330	3940
		+20～+80℃	7960	4850	4000	5610	2550	3600	4000	8030	6050
Characteristics.			Middle ε_{33}^T	General-purpose	High k_{33} & d_{33}		Low temp. coefficient	High Tc	High k_{33} & d_{33}	High ε_{33}^E Low Qm	Middle ε_{33}^E

※Material characteristics test method, except for a part of the characteristics, comply with the standard of Japan Electronics and Information Technology Industrial Association JEITA EM-4501A.

Figure 26 Properties of C-6 PZT patch (Products by Digital book, 2018)

The strain energy of the trapezoidal beam is seen using static structural analysis in Ansys and the result is shown in following figure.

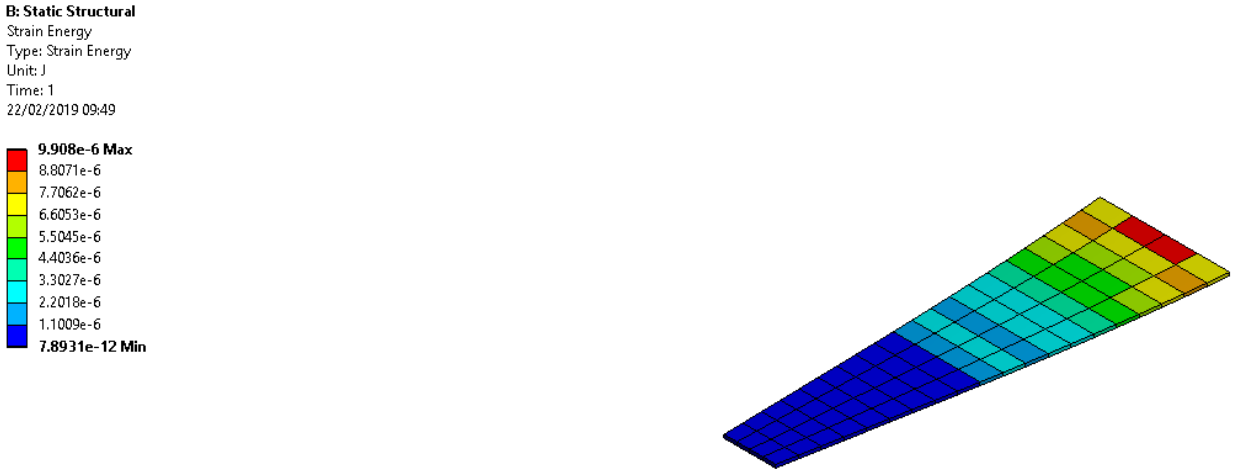

Figure 27 Strain Energy of the Harvester

It can be seen that the maximum energy is present near the base of the beam even though the beam is trapezoidal so the best place to attach a piezoelectric patch on a beam is near the base, the dimensions of the beam are quite large so not the entire structure is coupled only the partial structure of the beam is coupled.

4.3 Modal Analysis

After conducting the modal analysis of the beam in Ansys, the fundamental natural frequency of the coupled system is at 117.31 Hz, the higher frequencies are given in the following table.

Mode	Frequency [Hz]
1.	117.31
2.	541.15
3.	1123.2
4.	1441.4
5.	2513.8
6.	2762.4

The 1st,2nd and 3rd mode of vibration of the beam harvester is shown in the following figures.

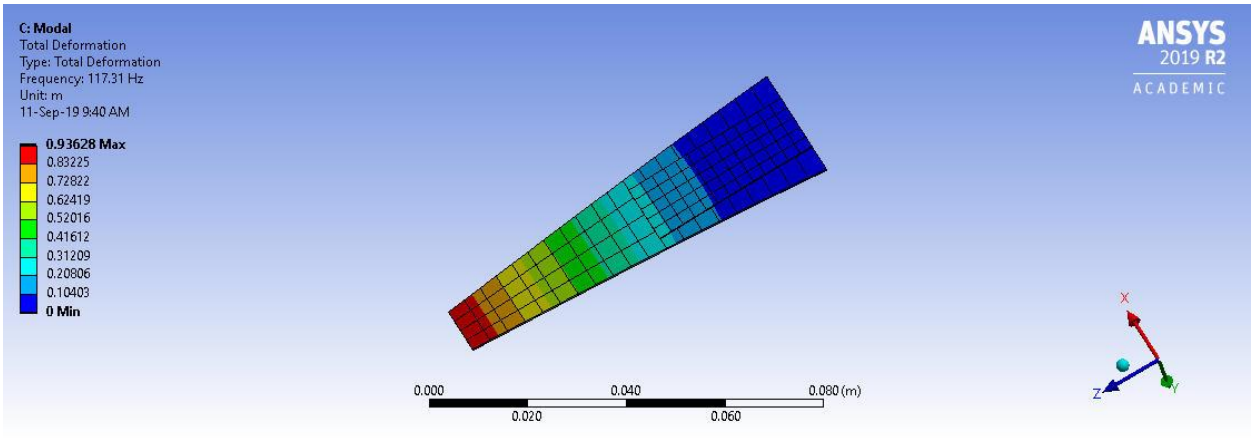

Figure 28 1st mode resonance frequency 117.31Hz

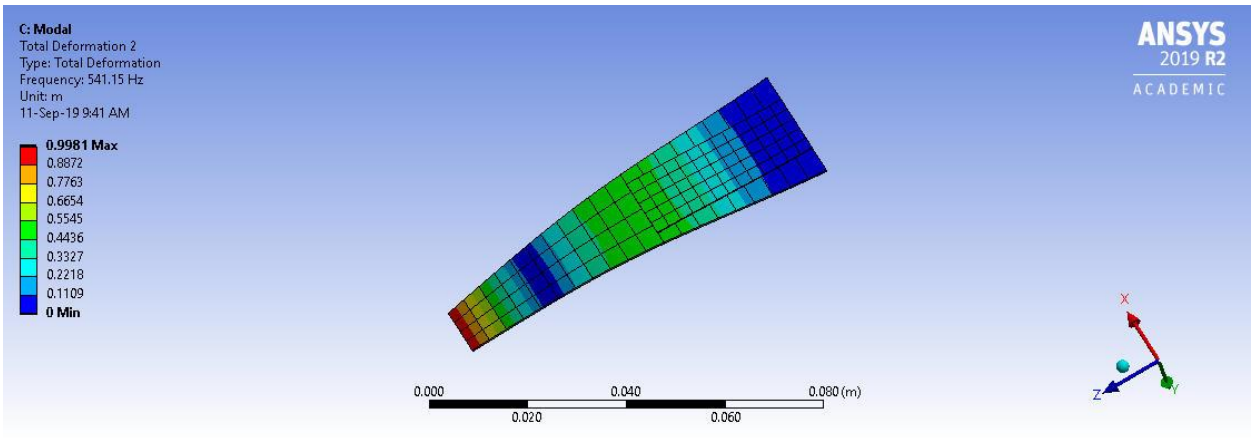

Figure 29 2nd mode resonance frequency 541.15

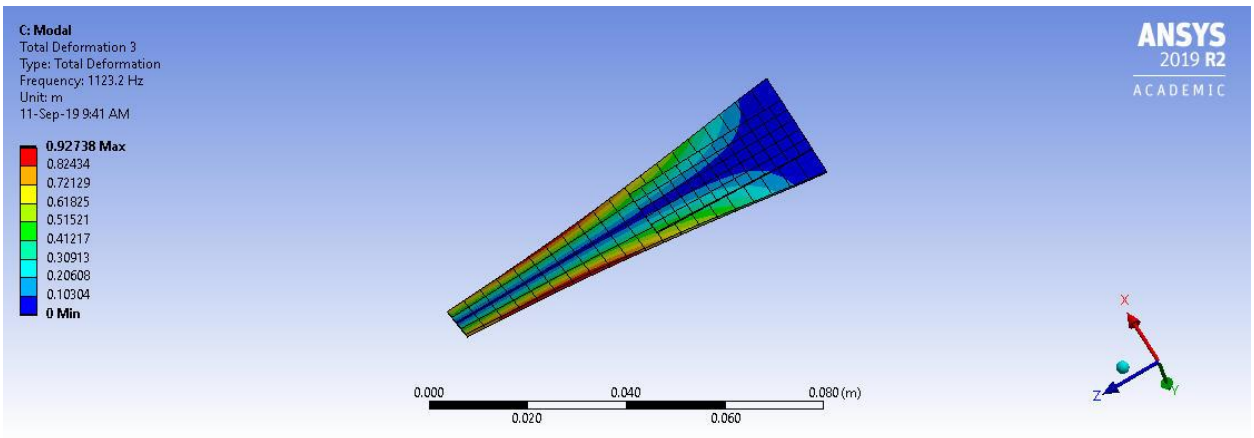

Figure 30 3rd mode resonance frequency 1441.4

The Harmonic analysis is performed in Ansys with the input acceleration of 1 g applied to the system in the z direction and the Frequency sweep of 0-1000Hz and the response is noted as in the accompanying graph.

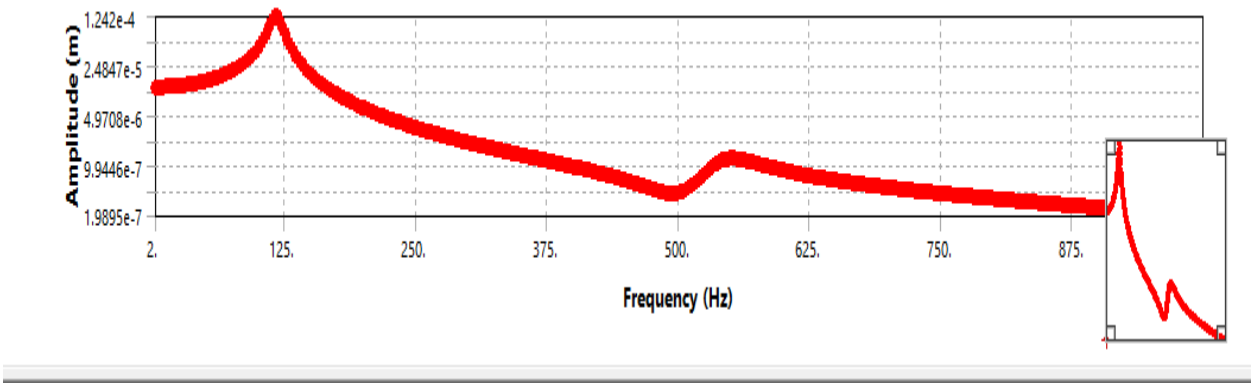

Figure 31 Frequency response of a cantilever harvester

The clear jump in a graph can be seen at 117.31Hz at first natural frequency where the resonance occurs and the 2nd jump is seen at 541.5Hz. The cantilever beam and the piezoelectric patch are coupled through a command in Ansys ADPL. The command is written in Ansys workbench to connect the model from workbench to the Mechanical ADPL and to read the voltage output.

4.4 Mechanical ADPL command

The following command was written in the Workbench to do the Post processing in the ADPL and to form the electrodes in the top and bottom layer of the Piezoelectric patch and to couple the Cantilever beam and the Piezo patch.

```
/prep7
allsel
cmsel,s,pbot
cp,1,volt,all
*get,nbot,node,0,num,min
cmsel,u,pbot
allsel
cmsel,s,ptop
cp,2,volt,all
*get,ntop,node,0,num,min
cmsel,u,ptop
et,5,circu94,0
r,5,1000
type,5
type,5$real,5
```

```
e,ntop,nbot
allsel
finish
/solve!
```

The Resistance load can be connected to the Harvester by the CIRCU94 (Coupled Field Analysis) command. 3 resistance values were chosen, and the results were recorded successively for the 3 and compared that at which resistance value the system works optimally. The upper body of the piezoelectric patch is coupled with the command CP and the electrode is formed at only one node, similarly the lower body is coupled to make another electrode and a resistor can be connected along these electrodes with the help of CIRCU94 command. The couple dofs in Ansys ADPL are shown in following figure.

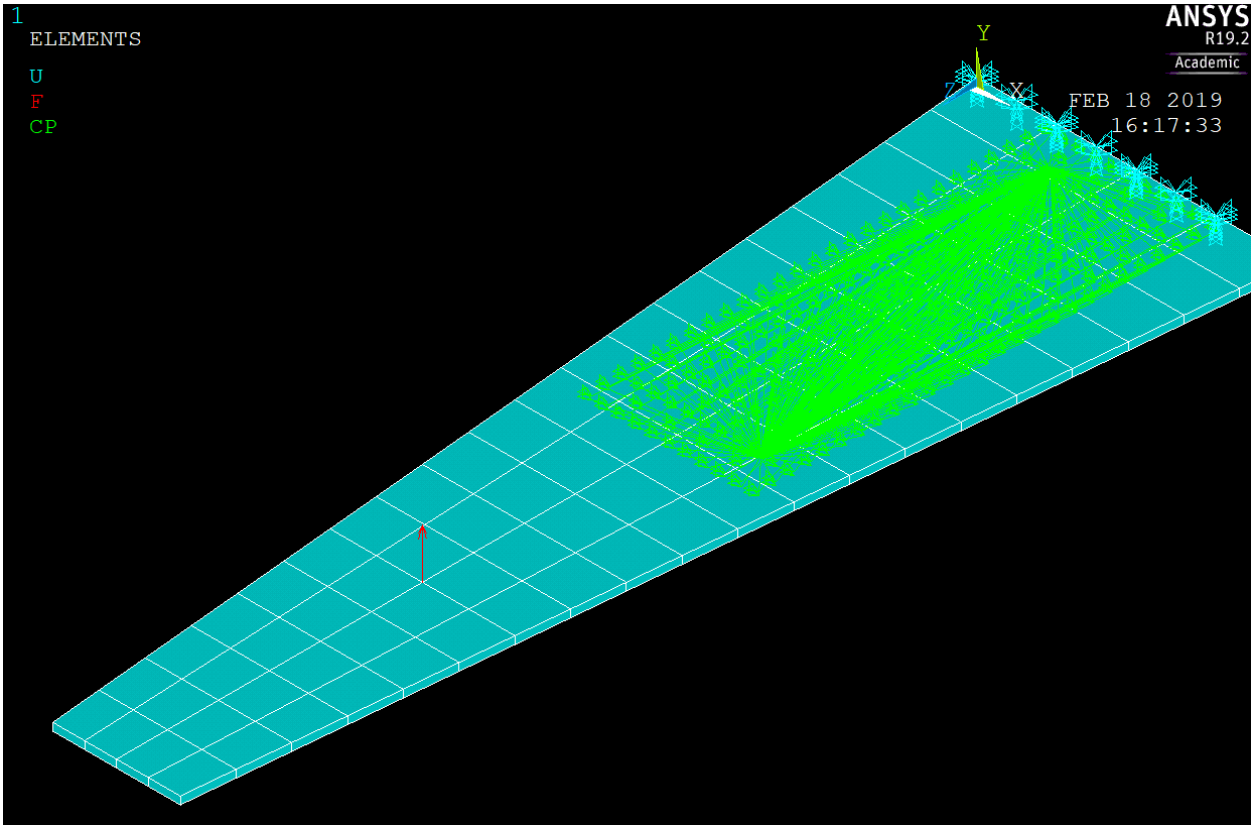

Figure 32 The coupling of DOFs in of Piezoelectric patch

It can be seen that all the nodes are connected to one node at the top of piezo body as well as bottom of the body to form an electrode. The electric potential can be read at these nodes and then the difference between the upper and the bottom node is the voltage output which is available to the resistor and is available to the applications. The input acceleration in this case is 10 m/s^2

The voltage response to the acceleration of 10 m/s^2 in Ansys mechanical ADPL using the above command can be seen by \post26 command and is shown in the following figures at different resistance values.

The resistance value can be changed with the CIRCU94 command provided by Ansys and the simulation can be solved again. It can be used to model resistance, inductance, capacitance, independent current and voltage source. and the simulation can be solved again. Ansys piezoelectric circuit elements cannot be used to model nonlinear elements such as diodes. So, the electric circuit is represented by the resistor attached to piezoelectric FE model and the power can be read. The results for voltage, power and current flow for the different resistance values of 1000, 10000 and 100000 ohms are recorded.

4.5 Voltage output and Power Harvested

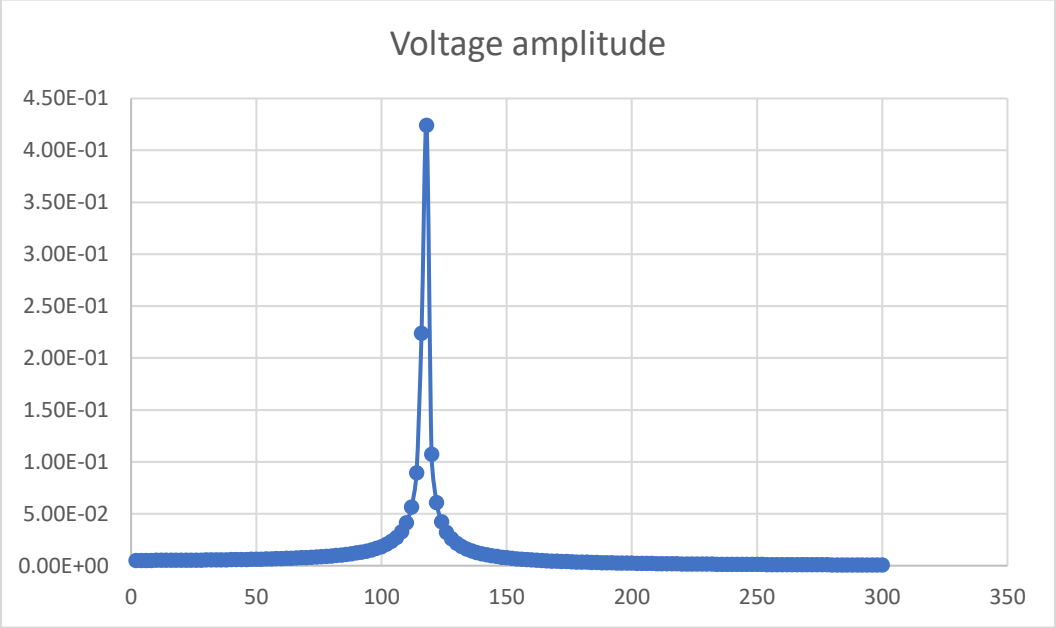

Figure 33 The voltage output at 1000 ohms resistor.

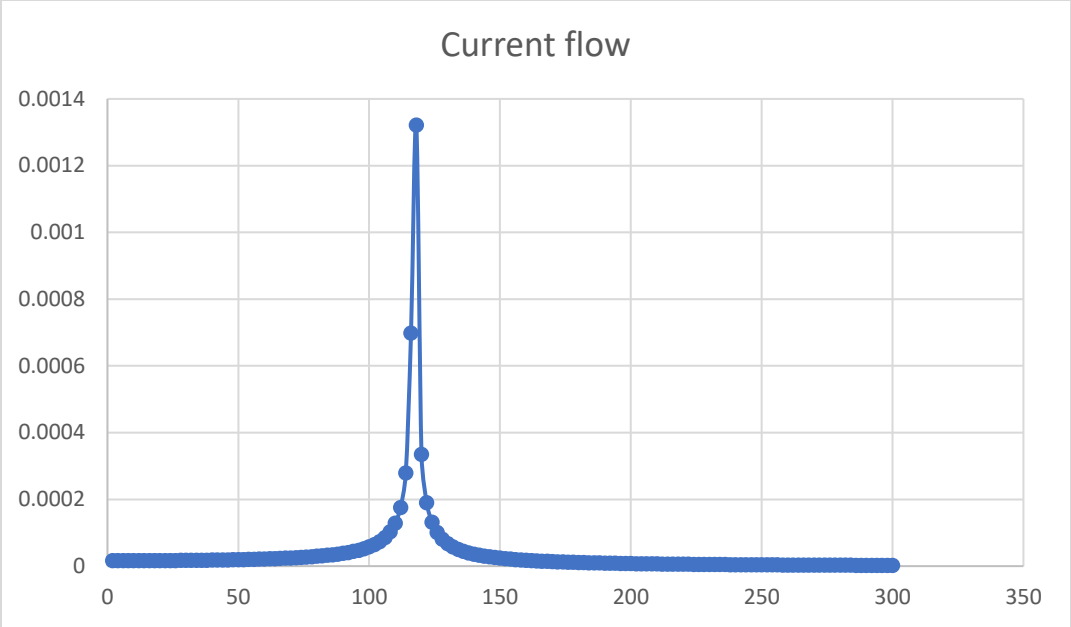

Figure 34 Current flow at 1000 ohms

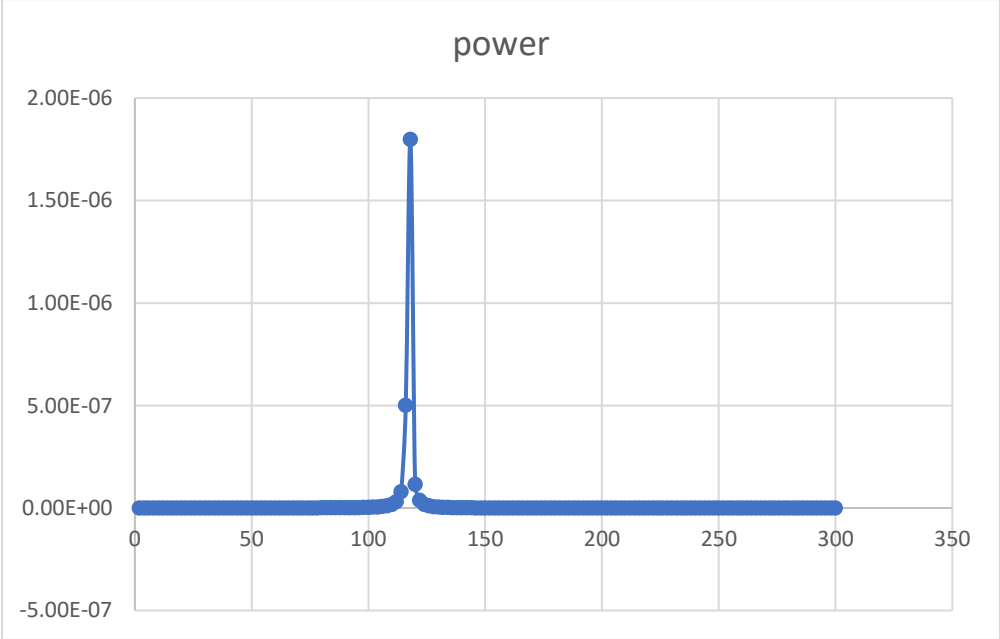

Figure 35 Power harvested at 1000 ohms

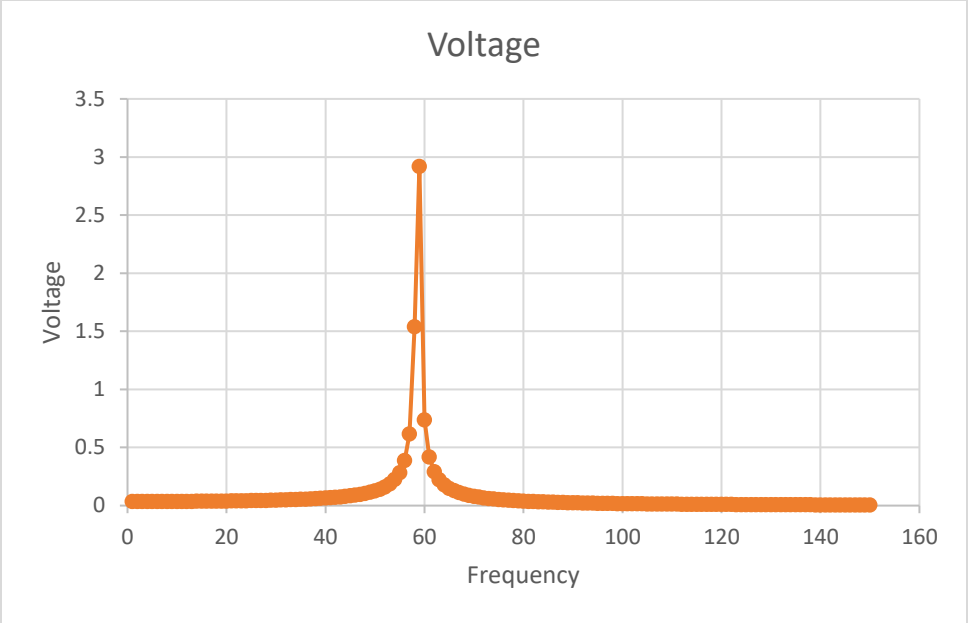

Figure 36 The Voltage output at 10K ohms

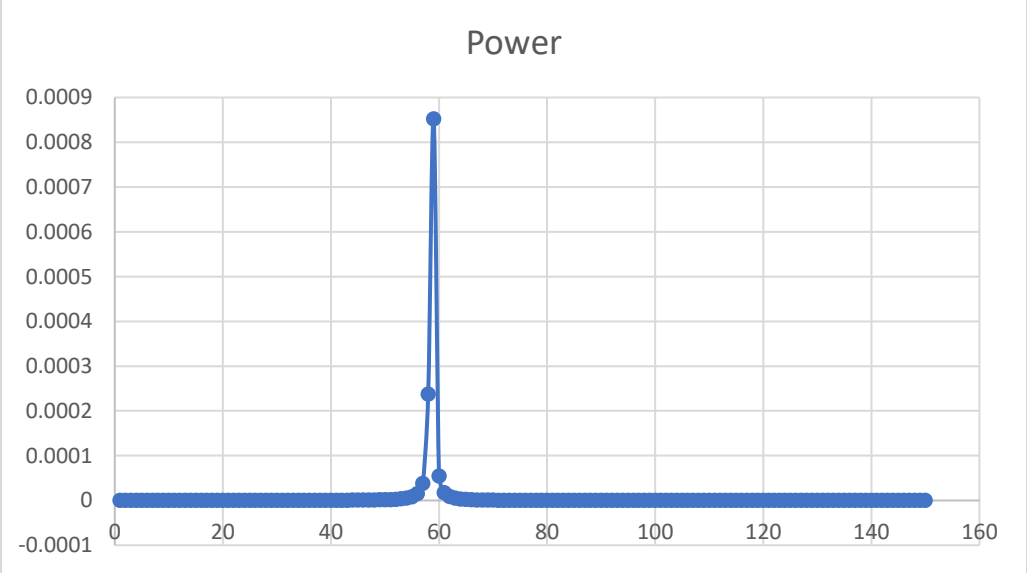

Figure 37 Power Harvested at 10K ohms

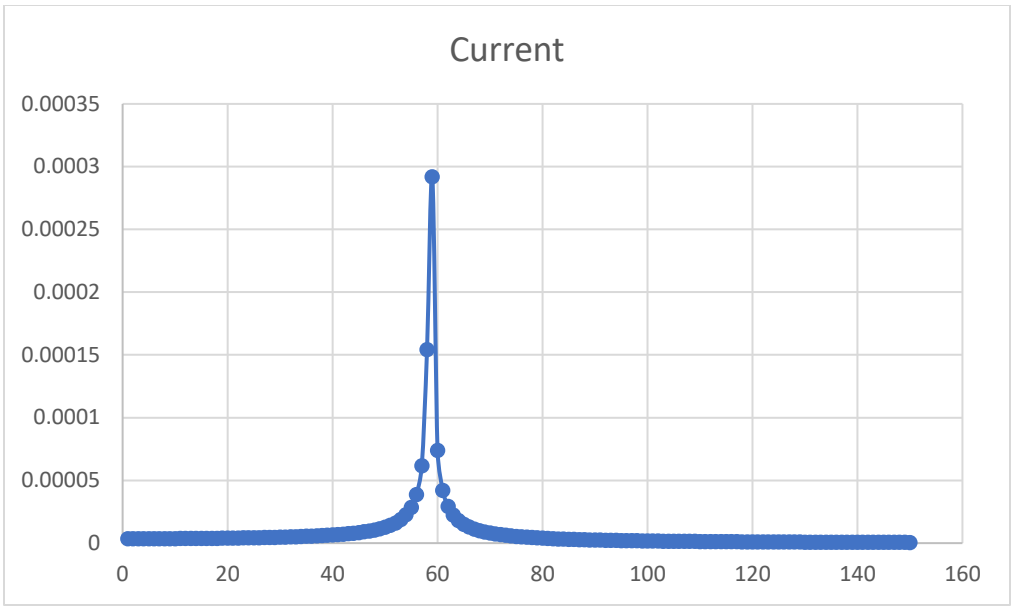

Figure 38 Current flow at 10K ohms

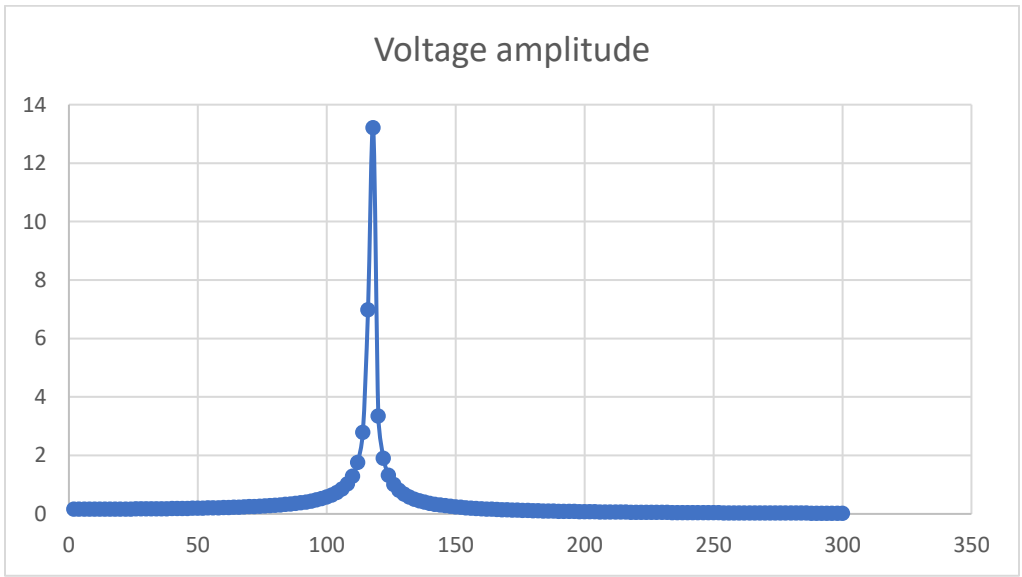

Figure 39 Voltage output at 100K ohms

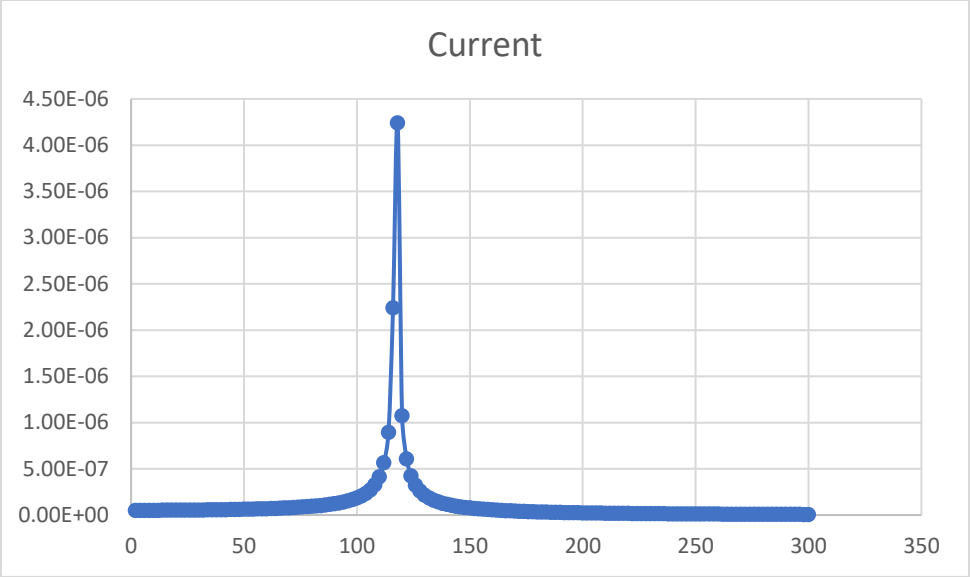

Figure 40 Current flow through 100K ohms resistor

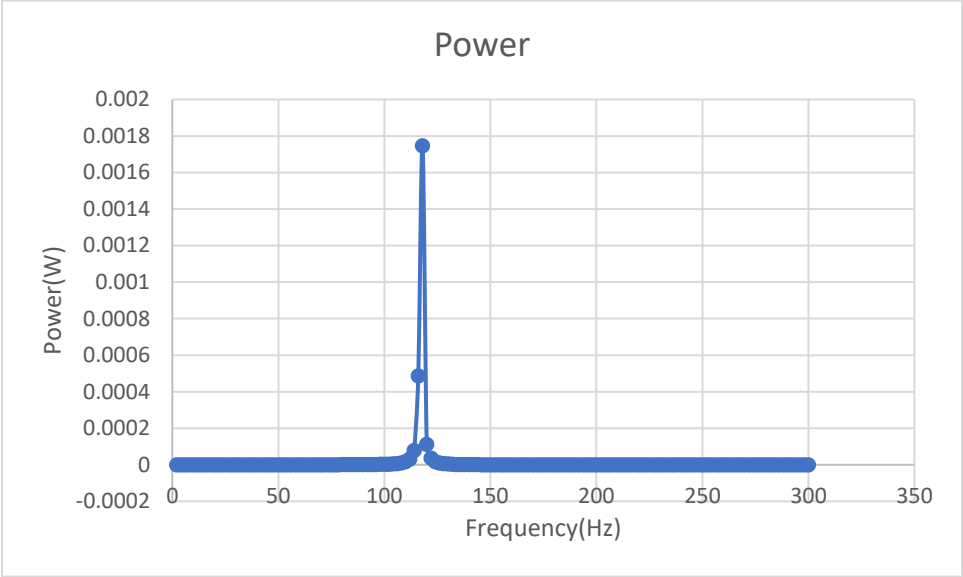

Figure 41 Power Harvested at 100K ohms

Out of the 3 resistors the best result was recorded at 100K ohm for the power, the voltage however is maximum at the highest resistance as the harvester moves towards the open circuit conditions and the current generated becomes less and less. The power harvested is of the order of few milliwatts which is suitable for certain applications of MEMS. The process to find the optimal resistance is called Impedance matching and helps to find the maximum power harvested in the given system. Of course, the maximum power is achieved at the resonance frequency, but still the viscous damping is considerably higher than the power harvested.

In the above figure's voltage, power and current flow vs frequency are plotted for different values of resistances. I00K ohm is the best solution to extract power for given system, as the power harvested is maximum and can be used to power micro devices, it can be further optimized by modeling the equivalent power harvesting electronic circuit and processing the power obtained.

4.6 Shape Optimization

The major problem with this technology is that the bandwidth of frequency for energy harvesting is very narrow and the ambient vibrations should vibrate exactly at the resonance frequency of the harvester, however, the vibrations present in the atmosphere are totally random and the vibrations are of very wide range. Researchers have proposed various solutions to minimize this problem. One of the solutions is to use comb type (Muthalif, 2014) cantilever beam so that the resonance phenomenon occurs at relatively close range of frequencies with respect to the single cantilever beam. As an example, one cantilever beam with beams of different sizes attached to it is modeled in Ansys to check the frequency response of the structure and the results are shown in following figures.

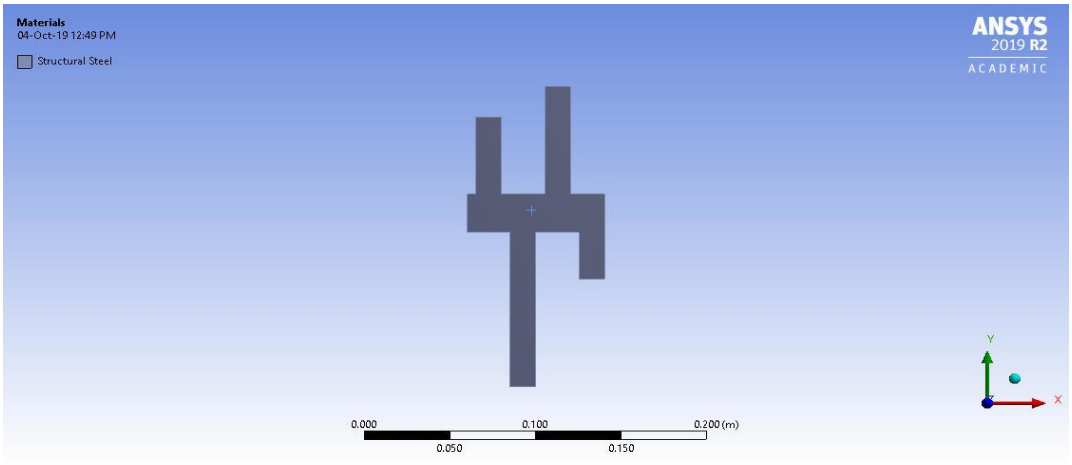

Figure 42 Comb type cantilever beam

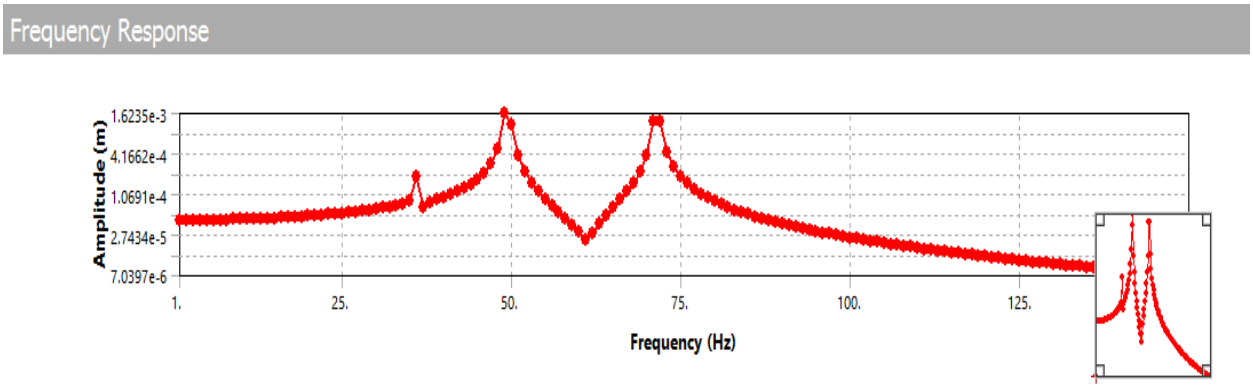

Figure 43 Frequency response to the force of 5N

5. Conclusions

Reduction of the power requirement of small electronic components made it possible to build self-powered sensors by harvesting the ambient vibration energy. Among several harvesting mechanisms to convert ambient vibration to electrical energy, piezoelectric energy harvesting received the greatest attention by researchers due to their larger power densities. Considering the advancements and the needs in piezoelectric energy harvesting, this thesis presents the methodology of modeling of Piezoelectric energy harvester using ANSYS software using different shape than the conservational shapes and read the output of certain electrical parameters like voltage, power and current.

In chapter 1 the introduction to the technology is summarized. In chapter 2 the theory about Wireless sensor nodes and a brief description of the working of these devices is provided and how these sensors are becoming essential in so many field of engineering and can help in certain applications.

In chapter 3 different type of energy harvesting techniques using ambient vibrations are discussed and compared and the technique to work on is decided keeping in mind all the advantages and disadvantages.

In chapter 4 the theory of energy harvesting technique and certain mathematical modeling techniques are discussed, and a system is selected to model, and the results are shown and discussed in detail. The voltage and power output are obtained by changing electrical and parameters of the system. The voltage output under different operating conditions is calculated and the optimal resistance for harvesting maximum power is calculated. The maximum voltage calculated in SDOF system is 4.4V and the maximum power harvested is 5mW.

In the 5^{th} chapter the finite element modeling of a trapezoidal cantilever harvester is performed using FEM tool ANSYS workbench. The piezoelectric patch is attached with the vibrating cantilever and the modal analysis is performed to find the natural frequencies and the harmonic analysis is performed to find displacement frequency response of the harvester. This analysis is performed with the help of Piezo and MEMs extension to the Ansys. Further, the electrodes are formed by coupling the nodes at the top and the bottom surface of the piezoelectric patch. The resistor can be connected to these electrodes and the voltage output is simulated for different operating conditions. The power calculated is of order of few milliwatts, so it is usable for different applications such as monitoring structures and certain other applications.

Bibliography

A. Eturk, D. i. (2008). A Distributed Parameter Electromechanical Model for Cantilevered Piezoelectric Energy Harvesters. *Journal of Vibrations and acoustics*.

Calio, R. (2014). Piezoelectric Energy Harvesting Solutions. *Mdpi*.

Cottone, F. (2011). *Introduction to Vibration Energy Harvesting.* August.

Coupled Field Analysis. (n.d.). Retrieved from http://read.pudn.com: http://read.pudn.com/downloads138/ebook/589790/gcou100.pdf

Holger, K., Willig, A., & Wolisz, A. (2004). Wireless sensor Networks. In K. Holger, A. Willig, & A. Wolisz, *Wireless sensor Networks* (pp. 4-11). Berlin: Springer.

Jessy L Baker, Shad Roundy,. (2005). Alternative Geometries for Increasing Power Density in Vibration Energy Scavenging for Wireless Sensor Networks. *Semantic Scholar*.

Muthalif, A. G. (2014). Optimal piezoelectric beam shape for single and broadband vibration energy harvesting: Modeling, simulation and experimental results. *Sciencedirect*.

Products by Digital book. (2018). Retrieved from Fuji Ceramics Corporation: http://www.fujicera.co.jp/managed/wp-content/themes/fujicera/digitalbook/en/elements/index_h5.html#3

Raghunathan, V., Schurgers, C., Park, S., & Srivastava, M. (2002). Energy-aware wireless microsensor networks. *IEEE*.

S. Bradai, S. N. (2018). Electromagnetic Vibration Energy Harvesting for Railway Applications. *Researchgate*, February.

Srivastava, M. (2002). *Sensor Node Platforms & Energy Issues*. Retrieved from https://slideplayer.com: https://slideplayer.com/slide/6341471/

Toit, N. E. (2005). *Modeling and Design of a MEMS Piezoelectric Vibration Energy Harvester .* Massachusets: MIT.